

Optimizing Utility-Energy Efficiency for the Metaverse over Wireless Networks under Physical Layer Security

Jun Zhao, Xinyu Zhou, Yang Li, Liangxin Qian

Nanyang Technological University, Singapore

junzhao@ntu.edu.sg, {xinyu003, yang048, qian0080}@e.ntu.edu.sg

ABSTRACT

The Metaverse, an emerging digital space, is expected to offer various services mirroring the real world. Wireless communications for mobile Metaverse users should be tailored to meet the following user characteristics: 1) emphasizing application-specific perceptual utility instead of simply the transmission rate, 2) concerned with energy efficiency due to the limited device battery and energy intensiveness of some applications, and 3) caring about security as the applications may involve sensitive personal data. To this end, this paper incorporates application-specific utility, energy efficiency, and physical-layer security (PLS) into the studied optimization in a wireless network for the Metaverse. Specifically, after introducing utility-energy efficiency (UEE) to represent each Metaverse user's application-specific objective under PLS, we formulate an optimization to maximize the network's weighted sum-UEE by deciding users' transmission powers and communication bandwidths. The formulated problem belongs to the sum-of-ratios optimization, for which prior studies have demonstrated its difficulty. Nevertheless, our proposed algorithm 1) obtains the global optimum for the weighted sum-UEE optimization, via a transform to parametric convex optimization problems, 2) applies to any utility function which is concave, increasing, and twice differentiable, and 3) achieves a linear time complexity in the number of users (the optimal complexity in the order sense). Simulations confirm the superiority of our algorithm over other approaches. We explain that our technique for solving the sum-of-ratios optimization is applicable to other optimization problems in wireless networks and mobile computing.

KEYWORDS

Wireless networks, Metaverse, physical-layer security, resource allocation, utility-energy efficiency.

1 INTRODUCTION

The Metaverse [1] is regarded as the next generation of the Internet, which consolidates technologies including extended reality (XR), digital twin, and wireless communications. In 2021, Facebook changed its name to Meta, raising public interest in the Metaverse.

Mobile users typically access the Metaverse via wireless communications. It is important to optimize wireless networks to meet the attributes of Metaverse users, which we present next.

Permission to make digital or hard copies of all or part of this work for personal or classroom use is granted without fee provided that copies are not made or distributed for profit or commercial advantage and that copies bear this notice and the full citation on the first page. Copyrights for components of this work owned by others than ACM must be honored. Abstracting with credit is permitted. To copy otherwise, or republish, to post on servers or to redistribute to lists, requires prior specific permission and/or a fee. Request permissions from permissions@acm.org.

Conference'23, 2023, Washington, DC, USA

© 2023 Association for Computing Machinery.

ACM ISBN 978-1-4503-XXXX-X/18/06...\$15.00

<https://doi.org/XXXXXXXX.XXXXXXX>

Characteristics of Metaverse users. We identify the following traits for mobile users of the Metaverse.

- ① Users aim to maximize **application-specific perceptual utility** rather than simply the transmission rate. Traditional network optimization considers the Quality of Service (QoS), such as the transmission rate, which quantifies the objective performance of the system. For the Metaverse, humans are the main players, so the Quality of Experience (QoE) capturing the perceptual experience of users is a better metric than QoS. To this end, our utility model should be adjusted accordingly.
- ② Users care about **energy efficiency** due to the limited battery of mobile devices and energy intensiveness of some applications. For instance, Meta Quest 2 with a fully charged battery can last for just 2 hours for gaming or 3 hours for video watching [2].
- ③ Users are concerned with **security** since certain Metaverse applications may involve personal (e.g., biometric and health) data. Researchers at UC Berkeley have shown in [3] that many existing Metaverse applications are vulnerable to privacy breaches by an attacker who tries to infer users' sensitive information.

The Metaverse over wireless networks: Utility-energy efficiency optimization under physical-layer security. Since mobile users accessing the Metaverse are constrained by wireless communication resources, it is vital to tailor wireless networks to match the above characteristics of Metaverse users. We formalize an optimization problem about the utility-energy efficiency (UEE) under physical-layer security for the motivation discussed below, where UEE for each user is defined as the application-specific perceptual utility over energy consumption.

Energy efficiency (EE) plays a vital role in both the economy and the environment. A faster transmission rate providing a higher quality of experience for users will also increase energy consumption. Therefore, it is essential to build an energy-efficient Metaverse system. Nevertheless, it is not viable to emphasize energy saving overwhelmingly. The Metaverse will provide many digital services, and lower transmission speeds will affect users' access to profits and high-quality experiences. Hence, how to allocate the resources (e.g., the transmission power and bandwidth) in the network to maximize the weighted sum of all users' UEE is worth investigating, where each user's weight represents its priority in the optimization. The weighted sum-UEE optimization aims to save energy and improve the utilities for users, addressing "①" and "②" above.

For "③" above, the confidential data of Metaverse applications should be accessible to only the intended users instead of eavesdroppers. To this end, we aim to achieve physical-layer security to protect the information during transmission. Secrecy capacity is an important metric in physical-layer security. It refers to the communication rate that does not leak information to an eavesdropper. In order to keep the information of users from the eavesdroppers, we

extend our Metaverse energy efficiency problem to physical-layer security by considering the secrecy rate instead of the original rate.

Our **contributions** include problem formulation, a widely applicable optimization technique, and an optimal algorithm in terms of the solution quality and time-complexity order, as listed below.

- We **formulate the problem** of maximizing the weighted sum of users' utility-energy efficiency (PLE) under physical-layer security for the Metaverse, by deciding users' transmission powers and bandwidth allocation. To the best of our knowledge, this problem has not yet been studied in the literature, inside and outside of Metaverse research.
- The formulated problem belongs to the sum-of-ratios optimization, which is non-convex. We explain that the problem is difficult to solve even using the pseudoconcavity notion.
- Despite the challenges, we solve the problem and develop an algorithm, via the **technique** of transforming the sum-of-ratios to parametric convex optimization problems.
- Our proposed **algorithm**
 - obtains the **global optimum**,
 - applies to **any** utility function which is concave, increasing, and twice differentiable, and
 - allows **heterogeneous** utility-function types among the users,
 - runs in **linear** time with respect to the number of users, which means the **optimal complexity** in the order sense.
- Simulations demonstrate the superiority of our algorithm over other approaches in terms of the solution quality and time complexity. The utility functions used in the simulations are based on real-world datasets.
- We explain that our **technique** can go beyond our problem to handle functions of product or quotient terms in **general** mathematical optimization. We illustrate this by discussing example problems in wireless networks and mobile computing. Researchers can use our technique to solve difficult problems.

Roadmap. The rest of the paper is organized as follows. Section 2 provides related studies. In Section 3, we formulate the studied optimization problem. Section 4 presents the challenges in solving the problem. Section 5 elaborates on our algorithm which finds a global optimum of the problem. In Section 6, we discuss the application of our optimization technique to other problems. Simulation results are reported in Section 7. Section 8 concludes the paper.

2 RELATED WORK

We survey related research: energy efficiency and physical-layer security in Section 2.1, and wireless Metaverse in Section 2.2.

2.1 Energy efficiency optimization and physical-layer security in wireless networks

In wireless networks, the traditional notion of energy efficiency (EE) for a user is defined as the ratio of data rate over power consumption (i.e., the ratio of transmitted data size over energy consumption). Maximizing the weighted sum of EE (WSEE) is addressed in [4, 5]. Different from WSEE, the system EE in [6] is defined as the ratio of all users' sum rates over all users' sum power consumption.

EE, WSEE, and system EE above do not examine specific application requirements. Accommodating various applications requires the concept of utility-energy efficiency (UEE), which for a user is the

ratio of the application-specific rate-dependent utility over power consumption. UEE in our paper has also been investigated in [7], which adopts game theory to model an interference-constrained wireless network, where each user maximizes its own UEE by deciding its transmission power. Different from UEE defined for individual users, the system UEE in [8] results from dividing the sum of all users' rate-dependent utilities by the sum of all users' power consumption. This system UEE optimization in [8] deals with just one ratio, which is much easier than the sum-of-ratios optimization in our paper. Moreover, the optimization method of [8] is applicable to only the specific utility function $\kappa_n \ln r_n$ for data rate r_n and constant κ_n . Even just changing the utility function to $\kappa_n \ln(1 + r_n)$ will make [8]'s approach invalid; in particular, (18a) in [8] will be non-concave and non-convex after the above change. In contrast, our work applies to any utility function that is concave, increasing, and twice differentiable. Besides the above major differences, [8] considers interference-constrained wireless networks and optimizes only the transmission powers, while we adopt FDMA and jointly optimize the transmission powers and bandwidth allocation.

Next, we discuss the incorporation of physical-layer security (PLS) into EE optimization. Because the WSEE as the sum of ratios is more difficult to analyze than the system EE, existing studies incorporating PLS into EE typically investigate the system EE instead of WSEE, after replacing the achievable rates with secrecy rates, as shown in [9, 10]. Despite the above work on EE optimization under PLS, we are unable to find any prior work on UEE optimization under PLS and hence the problem of our paper is new.

2.2 Metaverse over wireless networks

Calibrating wireless networks for mobile users accessing the Metaverse is an emerging research topic. Recently, a number of papers on the topic have appeared in different venues: [11] in JSAC, co-authored by the first author of the current paper, [12] in JSAC, [13] in TWC, [14, 15] in TVT, and a survey paper [1] in COMST, where the meanings of the abbreviations can be found in the references.

Among the technical papers above, [11, 12, 15] adopt reinforcement learning to optimize wireless performance for the Metaverse, while [13, 14] utilize economic theories to incentivize users for improving the usage of semantic-aware sensing and coded distributed computing for wireless Metaverse. The current paper's co-authors have recently optimized wireless federated learning in [16] for the Metaverse via alternating optimization, which achieves neither local nor global optimum. In contrast, our technique of the current paper goes beyond UEE optimization under PLS. Using it in [16] will obtain a global optimum, based on our Section 6 later.

3 PROBLEM FORMULATION

In this section, we will present the system model and formalize the optimization problem.

3.1 System model and metrics

In our studied system, a base station acts as the Metaverse server for N legitimate users $U_n|_{n=1,\dots,N}$. There are also N eavesdroppers $E_n|_{n=1,\dots,N}$, where E_n tries to intercept the communication between U_n and the server. Fig. 1 illustrates our system.

Our problem is applicable to downlink and uplink communications between all legitimate users and the Metaverse server.

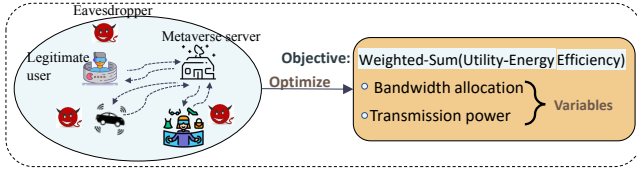


Figure 1: Our system: A server provides Metaverse services for N legitimate users $U_n|_{n=1,\dots,N}$, while the n th eavesdropper E_n tries to intercept the communication between user U_n and the server. The studied problem is to maximize the weighted sum of all users' utility-energy efficiency by deciding the bandwidth allocation and transmission powers.

Suppose the communications follow frequency division multiple access (FDMA), where different legitimate users' signals will not interfere with each other. For each legitimate user U_n , let B_n be the bandwidth, and p_n be its transmission power in the case of uplink communication, or the transmission power of the server used to communicate with U_n in the case of downlink communication. For simplicity, below we use uplink communication to introduce the problem. Throughout this paper, the n th dimension of an N -dimensional vector \mathbf{x} is denoted by x_n (unless stated otherwise). Hence, we have $\mathbf{p} := [p_1, p_2, \dots, p_N]$ and $\mathbf{B} := [B_1, B_2, \dots, B_N]$.

Transmission rate. According to the Shannon formula, the transmission rate $r_n(p_n, B_n)$ of legitimate user U_n is

$$r_n(p_n, B_n) = B_n \log_2 \left(1 + \frac{g_n p_n}{\sigma_n^2 B_n} \right), \quad (1)$$

where σ_n^2 is the power spectral density of Gaussian noise, g_n is the channel attenuation from U_n to the server. The function notation is used in this paper; e.g., $r_n(p_n, B_n)$ is a function of p_n and B_n .

Secrecy rate. Eavesdropper E_n aims to intercept the communication between legitimate user U_n and the server. Let $r_{n,e}$ be the eavesdropping rate of E_n . We consider $r_{n,e}$ as a constant depending on only n . Then the secrecy rate of U_n is given by

$$r_{n,s}(p_n, B_n) := r_n(p_n, B_n) - r_{n,e}. \quad (2)$$

Utility. We regard user U_n 's application-specific perceptual utility rate as a function of the secrecy rate $r_{n,s}(p_n, B_n)$ to emphasize physical-layer security (PLS). Specifically, using¹ $f_n(\cdot) : (0, \infty) \rightarrow (-\infty, \infty)$ to denote the utility rate function, user U_n 's utility rate is given by $f_n(r_{n,s}(p_n, B_n))$. Consider a small time interval $[t, t + \Delta t]$, where Δt is small enough such that $r_{n,s}(p_n, B_n)$ can be seen as invariant during $[t, t + \Delta t]$. Then the utility of user U_n over the time interval $[t, t + \Delta t]$ is $\mathcal{U}_n^{[t, t + \Delta t]} := f_n(r_{n,s}(p_n, B_n)) \Delta t$.

Power & energy consumption. The same as [8, 17], the power consumed by user U_n includes not just the transmission power p_n , but also the circuit power p_n^{cir} , which is a constant given n . During the time interval $[t, t + \Delta t]$, user U_n 's energy consumption is given by $\mathcal{E}_n^{[t, t + \Delta t]} := (p_n + p_n^{\text{cir}}) \Delta t$.

Utility-energy efficiency. For user U_n , we define its utility-energy efficiency (UEE) $\varphi_n(p_n, B_n)$ under PLS as the ratio of $\frac{\mathcal{U}_n^{[t, t + \Delta t]}}{\mathcal{E}_n^{[t, t + \Delta t]}}$ for small enough Δt , which induces

$$\varphi_n(p_n, B_n) := \frac{f_n(r_{n,s}(p_n, B_n))}{p_n + p_n^{\text{cir}}} = \frac{f_n(r_n(p_n, B_n) - r_{n,e})}{p_n + p_n^{\text{cir}}}. \quad (3)$$

¹We require $f_n(x)$ to be defined for any $x > 0$. We do not require $f_n(x)$ to be defined for $x = 0$, but if $\lim_{x \rightarrow 0^+} f_n(x)$ exists and is finite, we can just use it to define $f_n(0)$. We also do not enforce any condition on whether $f_n(x)$ is non-negative or not. Additional conditions of $f_n(x)$ are discussed in Section 4.2.

When $f_n(\cdot)$ becomes the identity function (i.e., $f_n(x) = x$), $\varphi_n(p_n, B_n)$ becomes $\frac{r_{n,s}(p_n, B_n)}{p_n + p_n^{\text{cir}}}$ (i.e., $\frac{\text{secrecy rate}}{\text{power consumption}}$), which is just the traditional notion of energy efficiency under PLS [18].

3.2 Utility-energy efficiency (UEE) optimization

Our goal is to maximize the weighted sum of all users' UEE under PLS. This optimization problem is formalized as follows:

$$\text{Problem } \mathbb{P}_1: \max_{\mathbf{p}, \mathbf{B}} \sum_{n \in \mathcal{N}} c_n \varphi_n(p_n, B_n) \quad (4)$$

$$\text{subject to: } \sum_{n \in \mathcal{N}} B_n \leq B_{\text{total}}, \quad (4a)$$

$$r_n(p_n, B_n) \geq r_n^{\min}, \text{ for all } n \in \mathcal{N} := \{1, \dots, N\}, \quad (4b)$$

where $c_n > 0$ represents the priority of user U_n in the optimization. Larger c_n means higher priority. Constraints (4a) sets the total bandwidth for FDMA. Constraint (4b) ensures that the transmission rate $r_n(p_n, B_n)$ of user U_n should be at least a constant r_n^{\min} (r_n^{\min} can vary for different n). Condition 1 below is about minimum legitimate rates $r_n^{\min}|_{n \in \mathcal{N}}$ and eavesdropping rates $r_{n,e}|_{n \in \mathcal{N}}$.

CONDITION 1. For all $n \in \mathcal{N}$, we have $r_n^{\min} \geq r_{n,e}$, $r_n^{\min} > 0$, $r_{n,e} \geq 0$.

We have the following remarks about Condition 1.

REMARK 1. Condition 1 with (4b) ensures $r_n(p_n, B_n) \geq r_{n,e}$; i.e., each user U_n 's secrecy rate $r_{n,s}(p_n, B_n)$ is non-negative.

REMARK 2. Condition 1 covers the following special case where we do not impose physical-layer security but still enforce a minimum transmission rate for each user: $r_{n,e} = 0$ and $r_n^{\min} > 0$ for all $n \in \mathcal{N}$.

REMARK 3. We enforce $r_n^{\min} > 0$ in Condition 1 so that each user U_n will always be allocated with a strictly positive bandwidth; i.e., $B_n > 0$ for all $n \in \mathcal{N}$. This avoids analyzing the degenerate case where only a subset of N users share the total bandwidth B_{total} .

We also comment on how Problem \mathbb{P}_1 is optimized in practice.

REMARK 4. Problem \mathbb{P}_1 will be solved using our Algorithm 1 in Section 5.2. Then a question is which entity solves \mathbb{P}_1 in practice. We let the Metaverse server perform the task, assuming that it has obtained the values of p_n^{cir} , r_n^{\min} , $r_{n,e}$ for all n (e.g., these are shared with the server before the optimization stage). After the server solves \mathbb{P}_1 , it will notify each legitimate user U_n of the p_n and B_n values.

4 CHALLENGES IN SOLVING PROBLEM \mathbb{P}_1

We first state the optimization preliminaries and conditions of the function $f_n(x)$, which are used to explain the difficulty in solving \mathbb{P}_1 .

4.1 Preliminaries of mathematical optimization

Let $f(\mathbf{x})$ be a function defined on a convex set \mathcal{S} , which is a subset of a real vector space. Then we have the following from Definitions 1.3.1, 2.2.1, and 3.2.1 of the book [19].

DEFINITION 1 (CONVEXITY). f is convex in \mathbf{x} if and only if for any $\mathbf{x}_1, \mathbf{x}_2 \in \mathcal{S}$ and $t \in [0, 1]$, it holds that $f(t\mathbf{x}_1 + (1-t)\mathbf{x}_2) \leq tf(\mathbf{x}_1) + (1-t)f(\mathbf{x}_2)$.

DEFINITION 2 (PSEUDOCONVEXITY). f is pseudoconvex in \mathbf{x} if and only if for any $\mathbf{x}_1, \mathbf{x}_2 \in \mathcal{S}$, $f(\mathbf{x}_1) > f(\mathbf{x}_2)$ implies $\nabla f(\mathbf{x}_1) \cdot (\mathbf{x}_2 - \mathbf{x}_1) < 0$, where ∇f denotes the gradient of f .

DEFINITION 3 (QUASICONVEXITY). f is quasiconvex in x if and only if for any $x_1, x_2 \in \mathcal{S}$ and $t \in [0, 1]$, it holds that $f(tx_1 + (1-t)x_2) \leq \max\{f(x_1), f(x_2)\}$.

With convexity above, Lemma 4.1 helps us understand concavity.

LEMMA 4.1 (CONVEXITY VERSUS CONCAVITY). A function f is said to be concave (resp., pseudoconcave, quasiconcave) if and only if $-f$ is convex (resp., pseudoconvex, quasiconvex).

For the reasoning behind Lemma 4.1, interested readers can refer to Section 3 of the book [19]. Lemma 4.2 below presents the relationships between the definitions discussed above.

LEMMA 4.2 (RELATIONSHIPS BETWEEN NOTIONS). With “ \Rightarrow ” denoting “implies”, we have the following assuming differentiability

$$\text{Convexity} \Rightarrow \text{Pseudoconvexity} \Rightarrow \text{Quasiconvexity}, \text{ and} \quad (5)$$

$$\text{Concavity} \Rightarrow \text{Pseudoconcavity} \Rightarrow \text{Quasiconcavity}. \quad (6)$$

Lemma 4.2 follows from Fig. 2.2 and Fig. B.1 of the book [19].

For a minimization problem, if the objective function and² the constraints are all convex, then we have a convex optimization problem, for which the following lemma holds.

LEMMA 4.3 (CHAPTERS 3 AND 4 OF [20]). For convex optimization, the Karush–Kuhn–Tucker (KKT) conditions are

- sufficient for optimality, and
- are necessary for optimality if Slater’s condition holds (i.e., if the feasible set contains at least one interior point).

Readers unfamiliar with the KKT conditions can refer to Theorem 4.2.3 of [19], and can also look into (11a)–(11l) to be presented on Page 5 of the current paper, where we will use the KKT conditions.

Lemma 4.4 below broadens problems under which KKT conditions are sufficient for optimality, to go beyond convex optimization.

LEMMA 4.4 (THEOREM 4.4.1 OF [19]). For a minimization problem with all constraints being inequalities, if the objective function is pseudoconvex, and all constraints are quasiconvex and differentiable, then a feasible point satisfying the KKT conditions is globally optimal.

4.2 Conditions of the utility function $f_n(x)$

The requirements of the utility rate function $f_n(x)$ for any $n \in \mathcal{N}$ are formally presented as Condition 2 below (we will just call $f_n(x)$ as the utility function hereafter for simplicity).

CONDITION 2. The utility function $f_n(x)$ for any $n \in \mathcal{N}$ is concave, increasing, and twice differentiable, with respect to $x > 0$; i.e., $f_n''(x) \leq 0$ and $f_n'(x) > 0$ for $x > 0$.

In Condition 2, the concavity of $f_n(x)$ means diminishing marginal return, which holds in various practical applications [21–24].

We also remark that $f_n(x)$, $f_n'(x)$ and $f_n''(x)$ are defined for any $x > 0$. Similar to Footnote 1, for any of $f_n(x)$, $f_n'(x)$ and $f_n''(x)$, we do not require it to be defined for $x = 0$. If it has a finite (resp., no) limit as $x \rightarrow 0^+$, we can just use the limit to define the corresponding value at $x = 0$ (resp., do not define any value at $x = 0$).

We can even allow heterogeneous types of utility functions among the users. For the specific expressions of the utility function $f_n(x)$ used in simulations, we will discuss three types in Section 7.1.

²Note that the constraint of a convex (resp., concave) function being at most (resp., least) a constant is a convex constraint.

We now discuss the properties of functions in our studied system.

LEMMA 4.5 (LEMMA 1 OF [16]). $r_n(p_n, B_n)$ is jointly concave with³ respect to p_n and B_n .

LEMMA 4.6. Under Condition 2, we have:

- $f_n(r_{n,s}(p_n, B_n))$ is jointly concave with respect to p_n and B_n ;
- $\varphi_n(p_n, B_n)$ is jointly pseudoconcave with respect to p_n and B_n .

PROOF. From Lemma 4.5 and Eq. (2), $r_{n,s}(p_n, B_n)$ is jointly concave in p_n and B_n . According to the composition rule in Eq. (3.11) of [20], for concave $f_n(\cdot)$, since $\tilde{f}_n(\cdot)$ defined as $f_n(\cdot)$ (resp., $-\infty$) for points inside (resp., outside) of the domain of f_n is non-decreasing, the function $f_n(r_{n,s}(p_n, B_n))$ is jointly concave in p_n and B_n .

From Page 245 (the book’s internal page number, not the pdf page number) of the book [19], for a ratio, if the numerator is non-negative, concave and differentiable, and the denominator is positive, convex and differentiable, then the ratio is pseudoconcave. Based on the above, we have proved the pseudoconcavity of $\varphi_n(p_n, B_n)$ with respect to p_n and B_n . \square

4.3 Challenges of solving Problem \mathbb{P}_1

Based on the proof of Lemma 4.6, we now call $\frac{f_n(r_{n,s}(p_n, B_n))}{p_n + p_n^{\text{cir}}}$ (i.e., $\varphi_n(p_n, B_n)$) a concave-convex ratio: a ratio having a concave function as the numerator and a convex function as the denominator. Then \mathbb{P}_1 is maximizing the sum of concave-convex ratios. Such sum-of-ratios optimization is non-convex and difficult to solve [25, 26].

Lemma 4.6 also shows that $\varphi_n(p_n, B_n)$ for each n is pseudoconcave, unfortunately the sum of pseudoconcave functions may not be pseudoconcave. Even if we manage to prove the pseudoconcavity of $\sum_{n \in \mathcal{N}} c_n \varphi_n(p_n, B_n)$ (the objective function of \mathbb{P}_1), which is very difficult (e.g., just analyzing the pseudoconvexity of the sum of two linear fractional functions is already challenging, as shown in [28]), then we can in principle use the KKT conditions of Problem \mathbb{P}_1 , as explained in⁴ Footnote 4, but those conditions involve taking derivatives of the ratios, inducing quite complex expressions, and the corresponding analysis becomes intractable. In this paper, instead of analyzing the pseudoconcavity of $\sum_{n \in \mathcal{N}} c_n \varphi_n(p_n, B_n)$ and being trapped in the intractable analysis, we will present an elegant approach (to be detailed in Section 5.1) for solving Problem \mathbb{P}_1 .

Recently, Shen and Yu [26, 27] proposed a novel technique to solve the sum-of-ratios optimization (referred to as fractional programming in their papers). However, since their technique relies on block coordinate ascent (i.e., alternating optimization), applying their technique to our Problem \mathbb{P}_1 will find a point which has no local or global optimality guarantee. In contrast, our approach will find a globally optimal solution of \mathbb{P}_1 .

5 ALGORITHM TO FIND A GLOBAL OPTIMUM

In this section, we will discuss how to transform \mathbb{P}_1 into a sequence of convex optimization problems, and then use the transform to propose an algorithm that finds a global optimum of \mathbb{P}_1 .

³For a function $f(\mathbf{x})$, “being convex (resp., concave) in \mathbf{x} ” has the same meaning as “jointly convex (resp., concave) in all dimensions of the vector \mathbf{x} ”.

⁴For \mathbb{P}_1 , all constraints are differentiable and convex (and hence quasiconvex) with Lemma 4.5 and Footnote 2. Hence, if we can prove that the objective function is pseudoconcave, Lemma 4.4 means that KKT conditions can solve \mathbb{P}_1 . Nonetheless, even if we can do the above, the KKT conditions of \mathbb{P}_1 are intractable to get a solution.

5.1 Transforming Problem \mathbb{P}_1 into parametric convex optimization problems

Firstly, we introduce an auxiliary variable β_n to transform Problem \mathbb{P}_1 into the epigraph form. Let $\frac{c_n f_n(r_{n,s}(p_n, B_n))}{p_n + p_n^{\text{cir}}} \geq \beta_n$ and \mathbb{P}_1 can be transformed to the following equivalent form as \mathbb{P}_2 :

$$\text{Problem } \mathbb{P}_2: \max_{\mathbf{p}, \mathbf{B}, \boldsymbol{\beta}} \sum_{n \in \mathcal{N}} \beta_n, \text{ where } \mathcal{N} := \{1, \dots, N\}, \quad (7)$$

$$\text{subject to: (4a), (4b),} \quad (7a)$$

$$F_n(p_n, B_n) - \beta_n \cdot (p_n + p_n^{\text{cir}}) \geq 0, \text{ for all } n \in \mathcal{N}, \quad (7b)$$

where we use $F_n(p_n, B_n)$ to simplify the representation:

$$F_n(p_n, B_n) := c_n f_n(r_{n,s}(p_n, B_n)). \quad (8)$$

Problem \mathbb{P}_2 is not convex optimization since $\beta_n \cdot (p_n + p_n^{\text{cir}})$ in (7b) is not jointly convex (actually also not jointly concave) in β_n and p_n , since the Hessian matrix for $\beta_n \cdot (p_n + p_n^{\text{cir}})$ is $\begin{bmatrix} 0 & 1 \\ 1 & 0 \end{bmatrix}$ which is not positive semidefinite (actually also not negative semidefinite).

We have explained in Section 4.3 that Problem \mathbb{P}_1 belongs to the following kind of problems: maximizing the sum of concave-convex ratios. Such problems have at least one global maximum according to [25, 26]. Hence, \mathbb{P}_1 and \mathbb{P}_2 have at least one global maximum.

To solve Problem \mathbb{P}_2 , one initial idea is trying to use Lemma 4.4 and hence the KKT conditions directly. Yet, deciding the quasi-convexity of $F_n(p_n, B_n) - \beta_n \cdot (p_n + p_n^{\text{cir}})$ in (7b) is very difficult. Hence, instead of trying to use \mathbb{P}_2 's KKT conditions directly, we take a step back and use the Fritz-John conditions (viz., Remark 4.2.2 of [19] and Lemma 2.1's proof in [25]), which do not need the quasi-convexity of constraints. The Fritz-John conditions provide the necessary conditions for a global optimum. Basically, in the Fritz-John conditions, the Lagrange multiplier (say w) on the gradient of the objective function can be zero or positive. Yet, following the proof of Lemma 2.1 in [25], we obtain $w > 0$. Then as shown in [25], w can be absorbed into other multipliers and hence omitted, after which the Fritz-John conditions reduce to the KKT conditions. Based on the above discussion, we have

$$\begin{aligned} &\text{any global maximum of } \mathbb{P}_2 \text{ needs to satisfy} \\ &\text{the KKT conditions (11a)–(11l) below.} \end{aligned} \quad (9)$$

For Problem \mathbb{P}_2 , with $\mathbf{v} := [v_n]_{n \in \mathcal{N}}$, $\boldsymbol{\tau} := [\tau_n]_{n \in \mathcal{N}}$ and λ denoting the multipliers, and the Lagrangian function given by

$$\begin{aligned} L_{\mathbb{P}_2}(\mathbf{p}, \mathbf{B}, \boldsymbol{\beta}, \mathbf{v}, \boldsymbol{\tau}, \lambda) &= -\sum_{n \in \mathcal{N}} \beta_n + \sum_{n \in \mathcal{N}} v_n \cdot (\beta_n \cdot (p_n + p_n^{\text{cir}}) - F_n(p_n, B_n)) \\ &\quad + \sum_{n \in \mathcal{N}} \tau_n \cdot (r_n^{\text{min}} - r_n) + \lambda \cdot (\sum_{n \in \mathcal{N}} B_n - B_{\text{total}}), \end{aligned} \quad (10)$$

the KKT conditions of Problem \mathbb{P}_2 are as follows, with $L_{\mathbb{P}_2}$ short for $L_{\mathbb{P}_2}(\mathbf{p}, \mathbf{B}, \boldsymbol{\beta}, \mathbf{v}, \boldsymbol{\tau}, \lambda)$ (see [19, Theorem 4.2.3] or [20, Section 1.4.2] for a formal introduction to the KKT conditions):

Stationarity:

$$\frac{\partial L_{\mathbb{P}_2}}{\partial p_n} = 0, \text{ for all } n \in \mathcal{N}, \quad (11a)$$

$$\frac{\partial L_{\mathbb{P}_2}}{\partial B_n} = 0, \text{ for all } n \in \mathcal{N}, \quad (11b)$$

$$\frac{\partial L_{\mathbb{P}_2}}{\partial \beta_n} = -1 + v_n \cdot (p_n + p_n^{\text{cir}}) = 0, \text{ for all } n \in \mathcal{N}; \quad (11c)$$

Complementary slackness:

$$v_n \cdot (\beta_n \cdot (p_n + p_n^{\text{cir}}) - F_n(p_n, B_n)) = 0, \text{ for all } n \in \mathcal{N}, \quad (11d)$$

$$\tau_n \cdot (r_n^{\text{min}} - r_n) = 0, \text{ for all } n \in \mathcal{N}, \quad (11e)$$

$$\lambda \cdot (\sum_{n \in \mathcal{N}} B_n - B_{\text{total}}) = 0; \quad (11f)$$

Primal feasibility:

$$F_n(p_n, B_n) - \beta_n \cdot (p_n + p_n^{\text{cir}}) \geq 0, \text{ for all } n \in \mathcal{N}, \quad (11g)$$

$$r_n(p_n, B_n) \geq r_n^{\text{min}}, \text{ for all } n \in \mathcal{N}, \quad (11h)$$

$$\sum_{n \in \mathcal{N}} B_n \leq B_{\text{total}}; \quad (11i)$$

Dual feasibility:

$$v_n \geq 0, \text{ for all } n \in \mathcal{N}, \quad (11j)$$

$$\tau_n \geq 0, \text{ for all } n \in \mathcal{N}. \quad (11k)$$

$$\lambda \geq 0. \quad (11l)$$

From (11c), it follows that

$$v_n = \frac{1}{p_n + p_n^{\text{cir}}}, \quad (12)$$

and (11j) holds.

Using (12) in (11d), we know

$$\beta_n = \frac{F_n(p_n, B_n)}{p_n + p_n^{\text{cir}}}, \quad (13)$$

and (11g) holds (actually the equal sign in (11g) is taken).

Instead of solving \mathbb{P}_2 's KKT conditions (11a)–(11l) directly, which is complex, we will connect them to a series of parametric convex optimization problems. In particular, supposing that $\boldsymbol{\beta}$ and \mathbf{v} are already given and satisfy (11c) (11d) (11g) and (11j), then we have the following result for the rest of \mathbb{P}_2 's KKT conditions:

(11a) (11b) (11e) (11f) (11h) (11i) (11k) and (11l), denoted by set \mathcal{K} , form the KKT conditions of Problem $\mathbb{P}_3(\boldsymbol{\beta}, \mathbf{v})$ below. (14)

where we have

$$\text{Problem } \mathbb{P}_3(\boldsymbol{\beta}, \mathbf{v}): \max_{\mathbf{p}, \mathbf{B}} \sum_{n \in \mathcal{N}} \mathcal{F}_n(p_n, B_n | \beta_n, v_n) \quad (15)$$

subject to: (4a), (4b).

with $\mathcal{F}_n(p_n, B_n | \beta_n, v_n)$ defined as follows:

$$\mathcal{F}_n(p_n, B_n | \beta_n, v_n) := v_n \cdot (F_n(p_n, B_n) - \beta_n \cdot (p_n + p_n^{\text{cir}})). \quad (16)$$

Lemma 5.1 below states the relationship between \mathbb{P}_2 and \mathbb{P}_3 .

LEMMA 5.1. *If we have ①: $[\mathbf{p}^*, \mathbf{B}^*, \boldsymbol{\beta}^*]$ is a globally optimal solution to Problem \mathbb{P}_2 , then we get ②: $\boldsymbol{\beta}^*$ denoting $[\beta_n^*]_{n \in \mathcal{N}}$ satisfies*

$$\beta_n^* = \frac{F_n(p_n^*, B_n^*)}{p_n^* + p_n^{\text{cir}}}, \text{ for all } n \in \mathcal{N}, \quad (17)$$

and ③: $[\mathbf{p}^*, \mathbf{B}^*]$ is a globally optimal solution to Problem $\mathbb{P}_3(\boldsymbol{\beta}^*, \mathbf{v}^*)$, where we have ④: \mathbf{v}^* denoting $[v_n^*]_{n \in \mathcal{N}}$ is given by

$$v_n^* = \frac{1}{p_n^* + p_n^{\text{cir}}}, \text{ for all } n \in \mathcal{N}. \quad (18)$$

PROOF. Problem $\mathbb{P}_3(\boldsymbol{\beta}, \mathbf{v})$ belongs to convex optimization. In particular, according to Lemma 4.6 and (8) (16), the objective function to be maximized is concave, while the constraints are clearly convex with Lemma 4.5 (note that “concave \geq constant” is a convex constraint as noted in Footnote 2). Also, Slater's condition holds for Problem $\mathbb{P}_3(\boldsymbol{\beta}, \mathbf{v})$. In other words, there exists at least one point $[\mathbf{p}, \mathbf{B}]$ such that constraints (4a) and (4b) are satisfied with strict inequalities. An example is as follows: with B_n being $\frac{B_{\text{total}}}{2N}$ for all $n \in \mathcal{N}$, set p_n such that $r_n(p_n, B_n) = 2r_n^{\text{min}}$ for all $n \in \mathcal{N}$. The above along with Lemma 4.3 shows the first “ \Leftrightarrow ” result below:

$$\begin{aligned} &\text{③} \Leftrightarrow [\mathbf{p}^*, \mathbf{B}^*, \boldsymbol{\beta}^*, \mathbf{v}^*] \text{ satisfies the set } \mathcal{K} \text{ of conditions in (14).} \\ &\quad \text{Results ② and ④ hold; i.e., } [\boldsymbol{\beta}^*, \mathbf{v}^*] \text{ satisfies (17) and (18).} \\ &\Leftrightarrow [\mathbf{p}^*, \mathbf{B}^*, \boldsymbol{\beta}^*, \mathbf{v}^*] \text{ satisfies KKT conditions (11a)–(11l)} \Leftrightarrow \text{①} \end{aligned} \quad (19)$$

where the second “ \Leftrightarrow ” above holds from (12) and (13), and the last “ \Leftarrow ” above follows from (9). \square

For additional understanding of Lemma 5.1, interested readers can refer to Lemma 2.1 and Remark 2.1 of [25], where Lemma 2.1 of [25] handles minimizing the sum of convex-concave ratios and Remark 2.1 of [25] maximizes the sum of concave-convex ratios.

With Lemma 5.1 presented above, we now describe how to solve Problem \mathbb{P}_2 using $\mathbb{P}_3(\boldsymbol{\beta}, \boldsymbol{\nu})$. Let $[\boldsymbol{p}^\#(\boldsymbol{\beta}, \boldsymbol{\nu}), \boldsymbol{B}^\#(\boldsymbol{\beta}, \boldsymbol{\nu})]$ denote a globally optimal solution to $\mathbb{P}_3(\boldsymbol{\beta}, \boldsymbol{\nu})$, where $\boldsymbol{p}^\#(\boldsymbol{\beta}, \boldsymbol{\nu}) = [p_n^\#(\boldsymbol{\beta}, \boldsymbol{\nu})]_{n \in \mathcal{N}}$ and $\boldsymbol{B}^\#(\boldsymbol{\beta}, \boldsymbol{\nu}) = [B_n^\#(\boldsymbol{\beta}, \boldsymbol{\nu})]_{n \in \mathcal{N}}$. We further define

$$\phi_{1,n}(\boldsymbol{\beta}, \boldsymbol{\nu}) := -F_n(p_n^\#(\boldsymbol{\beta}, \boldsymbol{\nu}), B_n^\#(\boldsymbol{\beta}, \boldsymbol{\nu})) + \beta_n \cdot (p_n^\#(\boldsymbol{\beta}, \boldsymbol{\nu}) + p_n^{\text{cir}}), \quad (20)$$

$$\phi_{2,n}(\boldsymbol{\beta}, \boldsymbol{\nu}) := -1 + \nu_n \cdot (p_n^\#(\boldsymbol{\beta}, \boldsymbol{\nu}) + p_n^{\text{cir}}), \quad (21)$$

$$\phi_1(\boldsymbol{\beta}, \boldsymbol{\nu}) := [\phi_{1,n}(\boldsymbol{\beta}, \boldsymbol{\nu})]_{n \in \mathcal{N}}, \quad \phi_2(\boldsymbol{\beta}, \boldsymbol{\nu}) := [\phi_{2,n}(\boldsymbol{\beta}, \boldsymbol{\nu})]_{n \in \mathcal{N}},$$

$$\phi(\boldsymbol{\beta}, \boldsymbol{\nu}) := [\phi_1(\boldsymbol{\beta}, \boldsymbol{\nu}), \phi_2(\boldsymbol{\beta}, \boldsymbol{\nu})]. \quad (22)$$

With $(\boldsymbol{p}^*, \boldsymbol{B}^*, \boldsymbol{\nu}^*)$ denoting a globally optimal solution to Problem \mathbb{P}_2 (and hence $(\boldsymbol{p}^*, \boldsymbol{B}^*)$ denoting a globally optimal solution to Problem \mathbb{P}_1), clearly setting $(\boldsymbol{\beta}, \boldsymbol{\nu})$ as $(\boldsymbol{\beta}^*, \boldsymbol{\nu}^*)$ of (17) and (18) satisfies

$$\phi(\boldsymbol{\beta}, \boldsymbol{\nu}) = \mathbf{0}. \quad (23)$$

Based on the above, solving Problem \mathbb{P}_2 and hence \mathbb{P}_1 can be transformed into solving (23) to obtain $\mathbb{P}_3(\boldsymbol{\beta}^*, \boldsymbol{\nu}^*)$, and then setting $[\boldsymbol{p}^*, \boldsymbol{B}^*]$ as $[\boldsymbol{p}^\#(\boldsymbol{\beta}^*, \boldsymbol{\nu}^*), \boldsymbol{B}^\#(\boldsymbol{\beta}^*, \boldsymbol{\nu}^*)]$, a globally optimal solution to $\mathbb{P}_3(\boldsymbol{\beta}^*, \boldsymbol{\nu}^*)$, according to Lemma 5.1. Based on the above idea, we present Algorithm 1 next, where it will become clear that solving \mathbb{P}_1 becomes solving a series of parametric convex optimization $\mathbb{P}_3(\boldsymbol{\beta}^{(i)}, \boldsymbol{\nu}^{(i)})$, with i denoting the iteration index. (24)

Readers may notice that our Lemma 5.1 provides just a necessary condition for a global optimum of Problem \mathbb{P}_2 . Lemma 5.2 below shows “necessary” and “sufficient” for strictly concave utility, which holds for all types of functions in simulations of Section 7.

LEMMA 5.2. *If the utility function $f_n(\cdot)$ for any $n \in \mathcal{N}$ is strictly concave (i.e., $f_n'(\cdot)$ is decreasing) for $x > 0$, the “ \Leftarrow ” in (19) can be replaced by “ \Leftrightarrow ”, so that “ $\textcircled{2} \textcircled{3} \textcircled{4}$ ” \Leftrightarrow “ $\textcircled{1}$ ” actually holds in Lemma 5.1.*

PROOF. From Theorem 2 on Page 7, for decreasing $f_n'(\cdot)$, we can prove that $\mathbb{P}_3(\boldsymbol{\beta}, \boldsymbol{\nu})$ has a **unique** global optimum $[\boldsymbol{p}^\#(\boldsymbol{\beta}, \boldsymbol{\nu}), \boldsymbol{B}^\#(\boldsymbol{\beta}, \boldsymbol{\nu})]$. We further obtain that $(\boldsymbol{\beta}^*, \boldsymbol{\nu}^*)$ satisfying (23) (i.e., “ $\textcircled{2} \textcircled{3} \textcircled{4}$ ”) is unique. Since we have explained that \mathbb{P}_2 has at least one global maximum, we know from the above this maximum is unique. Thus, for strictly concave utility, “ $\textcircled{2} \textcircled{3} \textcircled{4}$ ” \Leftrightarrow “ $\textcircled{1}$ ” holds in Lemma 5.1. \square

5.2 Our Algorithm 1 to solve Problem \mathbb{P}_1

As explained in the previous subsection, we solve (23) first in order to obtain a globally optimal solution to Problem \mathbb{P}_1 . Root-finding algorithms such as Newton’s method can be used to solve (23). Our Algorithm 1 actually uses a modified Newton method of [25], which always converges to the desired solution. In contrast, the original Newton’s method is sensitive to initialization (e.g., no convergence if starting at bad initialization, as shown in Section 4 of [25]).

Algorithm 1 starts with computing the initial $[\boldsymbol{\beta}^{(0)}, \boldsymbol{\nu}^{(0)}]$ from $[\boldsymbol{p}^{(0)}, \boldsymbol{B}^{(0)}]$, as shown in the pseudocode. In the i -th iteration of Algorithm 1 (i starts from 0), we update $[\boldsymbol{\beta}^{(i)}, \boldsymbol{\nu}^{(i)}]$ to $[\boldsymbol{\beta}^{(i+1)}, \boldsymbol{\nu}^{(i+1)}]$ based on (25) (26) (27) (28), which essentially present the modified Newton method to solve (23). The numerators in (26) (27) use $(\partial\phi_{1,n}(\boldsymbol{\beta}^{(i)}, \boldsymbol{\nu}^{(i)}))/(\partial\beta_n)$ and $(\partial\phi_{2,n}(\boldsymbol{\beta}^{(i)}, \boldsymbol{\nu}^{(i)}))/(\partial\nu_n)$, which are shown in Appendix A to be equal to

$$p_n^\#(\boldsymbol{\beta}^{(i)}, \boldsymbol{\nu}^{(i)}) + p_n^{\text{cir}}. \quad (29)$$

Algorithm 1: Our approach of computing a **globally optimal** solution $[\boldsymbol{p}, \boldsymbol{B}]$ (up to arbitrary accuracy) to Problem \mathbb{P}_1 of Section 3.2 on weighted sum-UEE optimization.

1 Initialize feasible $[\boldsymbol{p}^{(0)}, \boldsymbol{B}^{(0)}]$, $i = 0$, $\xi \in (0, 1)$, $\epsilon \in (0, 1)$.

2 Calculate $\boldsymbol{\beta}^{(0)} = [\beta_n^{(0)}]_{n \in \mathcal{N}}$ and $\boldsymbol{\nu}^{(0)} = [\nu_n^{(0)}]_{n \in \mathcal{N}}$ via

$$\beta_n^{(0)} = \frac{c_n f_n(r_{ns}(p_n^{(0)}, B_n^{(0)}))}{p_n^{(0)} + p_n^{\text{cir}}} \quad \text{and} \quad \nu_n^{(0)} = \frac{1}{p_n^{(0)} + p_n^{\text{cir}}}.$$

//Comment: Since we aim to find $(\boldsymbol{\beta}^*, \boldsymbol{\nu}^*)$ satisfying (23) (i.e., “ $\textcircled{2} \textcircled{3} \textcircled{4}$ ” in Lemma 5.1), the above initialization is intuitively good since it mimics (17) in “ $\textcircled{2}$ ” and (18) in “ $\textcircled{4}$ ” of Lemma 5.1.

3 **repeat**

4 Use Eq. (30) in Theorem 2 on Page 7 to solve $\mathbb{P}_3(\boldsymbol{\beta}^{(i)}, \boldsymbol{\nu}^{(i)})$, and obtain a solution $[\boldsymbol{p}^\#(\boldsymbol{\beta}^{(i)}, \boldsymbol{\nu}^{(i)}), \boldsymbol{B}^\#(\boldsymbol{\beta}^{(i)}, \boldsymbol{\nu}^{(i)})]$. //Comment: This line can use the bisection method in a straightforward manner, so we put the details in Appendix B.2.

5 Use $[\boldsymbol{p}^\#(\boldsymbol{\beta}^{(i)}, \boldsymbol{\nu}^{(i)}), \boldsymbol{B}^\#(\boldsymbol{\beta}^{(i)}, \boldsymbol{\nu}^{(i)})]$ obtained above to compute $\phi(\boldsymbol{\beta}^{(i)}, \boldsymbol{\nu}^{(i)})$ according to Eq. (22) on Page 6.

6 If $\phi(\boldsymbol{\beta}^{(i)}, \boldsymbol{\nu}^{(i)})$ is the zero vector, then

$[\boldsymbol{p}^\#(\boldsymbol{\beta}^{(i)}, \boldsymbol{\nu}^{(i)}), \boldsymbol{B}^\#(\boldsymbol{\beta}^{(i)}, \boldsymbol{\nu}^{(i)})]$ is the global optimal solution to Problem \mathbb{P}_1 and we finish the algorithm.

7 Otherwise, let J_i be the smallest integer that satisfies

$$\begin{aligned} & \|\phi(\boldsymbol{\beta}^{(i)} + \xi^{J_i} \boldsymbol{\sigma}_1^{(i)}, \boldsymbol{\nu}^{(i)} + \xi^{J_i} \boldsymbol{\sigma}_2^{(i)})\|_2 \\ & \leq (1 - \xi^{J_i} \epsilon) \cdot \|\phi(\boldsymbol{\beta}^{(i)}, \boldsymbol{\nu}^{(i)})\|_2, \end{aligned} \quad (25)$$

where “ $\|\cdot\|_2$ ” denotes the Euclidean norm, and the n th-dimension of $\boldsymbol{\sigma}_1^{(i)}$ (resp. $\boldsymbol{\sigma}_2^{(i)}$) for $n \in \mathcal{N}$, denoted by $\sigma_1^{(i)}[n]$ (resp. $\sigma_2^{(i)}[n]$), is given by

$$\sigma_1^{(i)}[n] := -\frac{(\partial\phi_{1,n}(\boldsymbol{\beta}^{(i)}, \boldsymbol{\nu}^{(i)}))/(\partial\beta_n)}{\phi_{1,n}(\boldsymbol{\beta}^{(i)}, \boldsymbol{\nu}^{(i)})} \quad (26)$$

$$= -\frac{(29)}{\text{RHS of (20) with } (\boldsymbol{\beta}, \boldsymbol{\nu}) \text{ being } (\boldsymbol{\beta}^{(i)}, \boldsymbol{\nu}^{(i)})},$$

$$\sigma_2^{(i)}[n] := -\frac{(\partial\phi_{2,n}(\boldsymbol{\beta}^{(i)}, \boldsymbol{\nu}^{(i)}))/(\partial\nu_n)}{\phi_{2,n}(\boldsymbol{\beta}^{(i)}, \boldsymbol{\nu}^{(i)})} \quad (27)$$

$$= -\frac{(29)}{\text{RHS of (21) with } (\boldsymbol{\beta}, \boldsymbol{\nu}) \text{ being } (\boldsymbol{\beta}^{(i)}, \boldsymbol{\nu}^{(i)})},$$

where RHS is short for the right-hand side.

//Comment: Obtaining J_i above involves evaluating $(J_i + 1)$ number of $\phi(\boldsymbol{\beta}, \boldsymbol{\nu})$ for (25). To compute each of them, we need to solve Problem $\mathbb{P}_3(\boldsymbol{\beta}, \boldsymbol{\nu})$ via (30) on Page 7 to obtain $[\boldsymbol{p}^\#(\boldsymbol{\beta}, \boldsymbol{\nu}), \boldsymbol{B}^\#(\boldsymbol{\beta}, \boldsymbol{\nu})]$, and then use (22).

8 Update

$$[\boldsymbol{\beta}^{(i+1)}, \boldsymbol{\nu}^{(i+1)}] \leftarrow [\boldsymbol{\beta}^{(i)} + \xi^{J_i} \boldsymbol{\sigma}_1^{(i)}, \boldsymbol{\nu}^{(i)} + \xi^{J_i} \boldsymbol{\sigma}_2^{(i)}], \quad (28)$$

where J_i is obtained from (25).

//Comment: If J_i happens to be 0, then (28) becomes the standard Newton method, as explained in the last paragraph on Page 13 of [25]. As shown by Problem 2 on Page 14 of [25], the standard Newton method may fail for some initial points, so we follow [25] to find J_i according to (25) instead of always setting J_i as 0.

9 Let $i \leftarrow i + 1$.

10 **until** $\phi(\boldsymbol{\beta}^{(i)}, \boldsymbol{\nu}^{(i)})$ is close to $\mathbf{0}$;

11 Use the current $[\boldsymbol{\beta}, \boldsymbol{\nu}]$ in (30) on Page 7 and return the obtained $[\boldsymbol{p}^\#(\boldsymbol{\beta}, \boldsymbol{\nu}), \boldsymbol{B}^\#(\boldsymbol{\beta}, \boldsymbol{\nu})]$ as the solution to Problem \mathbb{P}_1 .

The denominators in (26) (27) use $\phi_{1,n}(\boldsymbol{\beta}^{(i)}, \mathbf{v}^{(i)})$ and $\phi_{2,n}(\boldsymbol{\beta}^{(i)}, \mathbf{v}^{(i)})$, whose computations based on (20) (21) require obtaining $[\mathbf{p}^\#(\boldsymbol{\beta}^{(i)}, \mathbf{v}^{(i)}), \mathbf{B}^\#(\boldsymbol{\beta}^{(i)}, \mathbf{v}^{(i)})]$ by solving Problem $\mathbb{P}_3(\boldsymbol{\beta}^{(i)}, \mathbf{v}^{(i)})$. This is the reason why we have (24).

We remark that in Algorithm 1, the iterative process of computing $[\mathbf{p}^\#(\boldsymbol{\beta}^{(i)}, \mathbf{v}^{(i)}), \mathbf{B}^\#(\boldsymbol{\beta}^{(i)}, \mathbf{v}^{(i)})]$ and then using it for updating $[\boldsymbol{\beta}^{(i)}, \mathbf{v}^{(i)}]$ to $[\boldsymbol{\beta}^{(i+1)}, \mathbf{v}^{(i+1)}]$ is not the classical dual gradient descent (DGD) [20] despite the resemblance, since $\boldsymbol{\beta}$ is not a Lagrange multiplier. Algorithm 1 solves (23) using the modified Newton method, while DGD involves maximizing the dual function.

We formally state the solution quality of Algorithm 1 as follows.

THEOREM 1. *Under Conditions 1 and 2 of Section 4, our proposed Algorithm 1 finds a **globally optimal** solution to Problem \mathbb{P}_1 (up to arbitrary accuracy).*

PROOF. The analyses above in Sections 5.1 and 5.2, stated before Theorem 1, have already provided the proof of Theorem 1. \square

Next, we discuss the fast convergence and order-optimal time complexity of Algorithm 1. As shown in Theorem 3.2 of [25], the modified Newton method used in Algorithm 1 has global linear and local quadratic rates of convergence.

To analyze the time complexity, we use floating point operations (flops). One addition/subtraction/multiplication/division is one flop. We now analyze Lines 3–8, the main part of Algorithm 1. Suppose that in Line 4, we use the bisection method to obtain $\lambda^\#$ from (32), for which there are K iterations and each iteration has $\mathcal{O}(N)$, where K depends on the error tolerance, as detailed in Appendix B.2. Hence, Line 4 consumes $\mathcal{O}(KN)$. Lines 5, 6, and 8 cost $\mathcal{O}(N)$ flops. Line 7 takes $\mathcal{O}((J_i + 1)N)$ flops. Suppose the loop in Line 3 needs \mathcal{I} iterations before convergence (\mathcal{I} is less than 10 in our experiments to find a 0.01-global optimum, which means the relative difference between the objective-function values under the found solution and the true global optimum is at most 0.01). Then the time complexity of Algorithm 1 is $\mathcal{O}(\mathcal{I}KN + \sum_{i=0}^{\mathcal{I}-1} (J_i + 1)N)$, which is linear in N . This linear complexity is the best that any algorithm can do, since we need to decide N number of $[B_n, p_n]$ for all N users. Hence, Algorithm 1 achieves the optimal time complexity in the order sense.

5.3 Solving Problem $\mathbb{P}_3(\boldsymbol{\beta}, \mathbf{v})$

From (24), solving Problem \mathbb{P}_1 requires solving a series of $\mathbb{P}_3(\boldsymbol{\beta}, \mathbf{v})$. One approach is to use the Stanford CVX tool [20]. However, the worst-case complexity of global convex optimization grows exponentially with the problem size N from Section 1.4.2 of [20]. Based on Theorem 2 below, we can solve $\mathbb{P}_3(\boldsymbol{\beta}, \mathbf{v})$ and hence \mathbb{P}_1 in linear time with respect to N , as discussed in the previous subsection.

THEOREM 2. *Under Conditions 1 and 2 of Section 4, any **globally optimal** solution $[\mathbf{p}^\#(\boldsymbol{\beta}, \mathbf{v}), \mathbf{B}^\#(\boldsymbol{\beta}, \mathbf{v})]$ to Problem $\mathbb{P}_3(\boldsymbol{\beta}, \mathbf{v})$ defined in (15) can be given as follows:*

$$\begin{cases} B_n^\#(\boldsymbol{\beta}, \mathbf{v}) = \mathcal{B}_n(\lambda^\#) \text{ for all } n \in \mathcal{N}, \\ p_n^\#(\boldsymbol{\beta}, \mathbf{v}) = \frac{\sigma_n^2 B_n^\#(\boldsymbol{\beta}, \mathbf{v}) \cdot \psi_n(\lambda^\#)}{g_n} \text{ for all } n \in \mathcal{N}, \end{cases} \quad (30)$$

with function $\mathcal{B}_n(\lambda)$ defined by

$$\mathcal{B}_n(\lambda) := \frac{\max\{y_n(\lambda), r_n^{\min}\}}{\log_2(1 + \psi_n(\lambda))}, \quad (31)$$

and $\lambda^\#$ denoting the solution to

$$\sum_{n \in \mathcal{N}} \mathcal{B}_n(\lambda) = B_{\text{total}}. \quad (32)$$

where $\psi_n(\lambda)$ and $\gamma_n(\lambda)$ are defined by

$$\psi_n(\lambda) := \exp\left\{1 + W\left(\frac{1}{e} \left(\frac{g_n \lambda}{v_n \beta_n \sigma_n^2} - 1\right)\right)\right\} - 1, \quad (33)$$

for $W(\cdot)$ being the principal branch of the Lambert W function

($W(z)$ for $z \geq -e^{-1}$ is the solution of $x \geq -1$ to the equation $x e^x = z$),

$$\text{and } \gamma_n(\lambda) - r_{n,e} := \begin{cases} \xi := (f'_n)^{-1}\left(\frac{\beta_n \sigma_n^2 \cdot (1 + \psi_n(\lambda)) \ln 2}{c_n g_n}\right) \\ \text{when such result } \xi \geq 0 \text{ exists,} \\ 0, \text{ otherwise,} \end{cases} \quad (34)$$

with $(f'_n)^{-1}(\cdot)$ denoting the inverse function of the derivative $f'_n(\cdot)$.

Theorem 2 is proved in Appendix B, where we also elaborate on the bisection method to obtain $\lambda^\#$ from (32).

6 BROAD USAGE OF OUR TECHNIQUE

In this section, we review the optimization used in Algorithm 1 to obtain an insightful technique, which can be used to solve many other problems in wireless networks and mobile computing.

In Section 5.1, Problem \mathbb{P}_2 is not convex optimization since the non-convex product $\beta_n \cdot (p_n + p_n^{\text{cir}})$ exists in (7b), as shown in the sentences following (8). The solving process of \mathbb{P}_2 is transformed into solving a series of parametric convex optimization $\mathbb{P}_3(\boldsymbol{\beta}, \mathbf{v})$ where $[\boldsymbol{\beta}, \mathbf{v}]$ is given so that there is no non-convex product term and we have convex optimization. The solving of each \mathbb{P}_3 is used to update $[\boldsymbol{\beta}, \mathbf{v}]$ under which \mathbb{P}_3 is solved again with the new $[\boldsymbol{\beta}, \mathbf{v}]$, where the update of $[\boldsymbol{\beta}, \mathbf{v}]$ is based on the KKT conditions of \mathbb{P}_2 .

From the above discussion, we can identify the following:

Our technique to handle functions of product or quotient terms in optimization: With “ \ast ” denoting multiplication or division, if there are terms $f_n(A_n(\mathbf{x}) \ast y_n)_{n \in \mathcal{N}}$ in an optimization problem \mathbb{P} , for functions f_n, A_n, y_n and variables \mathbf{x} and $\mathbf{y} = [y_n]_{n \in \mathcal{N}}$, we can convert \mathbb{P} into a series of parametric convex optimization $\mathbb{Q}(\mathbf{y}, \mathbf{z})$, where \mathbf{z} comprises additional variables in the parameterization (e.g., \mathbf{v} in our “ $\mathbb{P}_3(\boldsymbol{\beta}, \mathbf{v})$ ”). In $\mathbb{Q}(\mathbf{y}, \mathbf{z})$, given $[\mathbf{y}, \mathbf{z}]$, variables in $A_n(\mathbf{x}) \ast y_n$ just have \mathbf{x} , so that \mathbb{Q} can be easier to solve than \mathbb{P} , or \mathbb{Q} may even happen to be convex in \mathbf{x} . The solving of each \mathbb{Q} will be used to update $[\mathbf{y}, \mathbf{z}]$ under which \mathbb{Q} is solved again with the new $[\mathbf{y}, \mathbf{z}]$, where the update of $[\mathbf{y}, \mathbf{z}]$ is based on the KKT conditions of \mathbb{P} .

With the above technique, we can address $f_n(A_n(\mathbf{x}) \ast B_n(\mathbf{x}))_{n \in \mathcal{N}}$ in optimization as well, for functions f_n, A_n, B_n and variables \mathbf{x} . We replace $A_n(\mathbf{x}) \ast B_n(\mathbf{x})$ by an auxiliary variable z_n and enforce the constraint of z_n being either no greater or no less than $A_n(\mathbf{x}) \ast B_n(\mathbf{x})$ (depending on the specific problem), where the constraint can be further converted into a relationship between $A_n(\mathbf{x})$ and $z_n \ast B_n(\mathbf{x})$, like how we transform \mathbb{P}_1 of (4) to \mathbb{P}_2 of (7).

To summarize, our technique can be useful for various optimization problems involving product or quotient terms. In addition, the technique often obtains a global optimum, as in Theorem 1. The above finding goes beyond the sum-of-ratios optimization of [25], although our original motivation comes from [25]. The following discussion shows that our above finding is very likely to be new.

Two recent papers [26, 27] by Shen and Yu have been considered breakthroughs in fractional programming, as seen from their high citations (692 and 190, respectively, as of 10 March 2023 in Google

Scholar). However, they find neither local nor global optimum. In contrast, our technique above will find a global optimum. Interested readers can refer to Appendix F.

Our above technique can be applied to many optimization problems in wireless networks and mobile computing, as illustrated by two examples below. In interference-constrained wireless networks, globally solving the weighted sum-rate maximization (WSRM) efficiently was an open problem for years before it was addressed by [30], since a user’s rate (per unit bandwidth) given by $\log_2(1 + \frac{\text{TransmitPower}}{\text{Interference+Noise}})$ involves a fraction inside a logarithm, which is difficult to deal with. Our technique above will find a global optimum for WSRM and other problems involving the above rate expression, while the polyblock-based approach of [30] relies on the structure of WSRM and may not be applicable to other problems. In mobile edge computing, with γ denoting the offloading ratio of computation tasks, [31] minimizes the system cost, given by $\gamma \cdot \text{EdgeComputingCost} + (1-\gamma) \cdot \text{LocalComputingCost}$. The multiplication above means no joint convexity in γ and other variables. Then [31] uses alternating optimization which is neither locally nor globally optimal, while our technique will find a global optimum.

7 SIMULATION

The utility functions for simulations are presented in Section 7.1 and validated by real data in Section 7.2. Then we describe simulation settings in Section 7.3, before reporting results in other subsections.

7.1 Utility functions for simulation

We provide three types of utility functions below since the Metaverse offers diverse applications. In Section 7.2, we validate these functions using real data.

Type 1 utility function: We have

$$f_n(x) = \kappa_n \ln(b_n + a_n x), \quad (35)$$

where $a_n, \kappa_n > 0, b_n \geq 0$. This type is used in [21] for sensing tasks. In simulations starting from Section 7.3, we let $b_n = 1$.

Type 2 utility function: We have

$$f_n(x) = \kappa_n \cdot (1 - e^{-a_n x + c_n}), \quad (36)$$

where $a_n, \kappa_n > 0$, and e denotes Euler’s number. This type is motivated by [22] on augmented reality. We let $c_n = 0$ in simulations.

Type 3 utility function: We have

$$f_n(x) = \kappa_n (x + d_n)^{a_n}, \quad (37)$$

where $\kappa_n > 0, d_n \geq 0$, and $0 < a_n < 1$. This function form has been used in prior work on congestion control [23] and mobile data subsidization [24]. We let $d_n = 0$ in simulations. In the terminologies of economics, $\kappa_n r_{n,s}^{a_n}$ can be viewed as a Cobb–Douglas utility with respect to $r_{n,s}$, while $\kappa_n \cdot (r_n - r_{n,e})^{a_n}$ can be regarded as a Stone–Geary utility with respect to r_n ; see Page 7 of [32].

It is straightforward to show that the above three types for the utility function all satisfy Condition 2 of Section 4.2. These three types are what we will use in simulations from Section 7.3. We emphasize that our theoretical results (e.g., Algorithm 1 as well as Theorems 1 and 2 in Section 5) of this paper apply to **any** utility function satisfying Condition 2 of Section 4.2.

7.2 Real data validating utility functions above

We now validate Section 7.1’s utility functions with the SSV360 [33] and Netflix datasets [34] from real-world experiments.

SSV360 dataset. This dataset of [33] captures users’ assessment of 360° videos when wearing HTC Vive Pro virtual reality headsets. Each data point represents a user’s subjective quality assessment of a 360° scene, under standing or seated viewing (SSV). In the dataset, having data points under different video bitrates yet the same resolution is due to different quantization parameters used in video compression. The wireless data rate should be large enough to ensure a smooth watching experience at the given video bitrate [22]. We let the bitrate be a constant fraction (say θ) of the wireless rate. Since changing the bitrate r_{bitrate} to the wireless rate r_{wireless} just involves replacing r_{bitrate} with $r_{\text{wireless}}/\theta$, we perform curve-fitting with the bitrate to validate the utility functions. The curves in Fig. 2(a) are for the scenarios of “user 1 seated”, “user 2 seated”, and “user 1 standing” respectively, to watch the same 360° scene “FormationPace” [33] with 2K resolution (i.e., 2048×1080 pixels).

In the SSV360 dataset, the score follows the widely used Absolute Category Rating (ACR) [35] and is an integer from 1 to 5. To obtain better curve-fitting results, we further use the Netflix dataset, where the score (i.e., the y -axis) ranges from 0 to 100.

Netflix dataset. In this dataset [34], which is a part of Netflix’s Emmy Award-winning Video Multimethod Assessment Fusion (VMAF) project, each data point exhibits users’ mean opinion score in $[0, 100]$ for a video at a given resolution and a given bitrate. Because there are not enough data points that have different bitrates yet the same resolution, we treat both resolution and bitrate as variables for curve-fitting. The results are shown in Fig. 2(b).

The expressions for the curves in Fig. 2 are in the table below.

Dataset	Scenario in [33] or video in [34]	Utility function from curve-fitting for normalized bitrate x and normalized resolution y explained in the caption of Fig. 2
SSV360 in [33]	user 1 seated	Type 1: $0.5424 \ln(1 + 37.2965x)$
	user 2 seated	Type 2: $2.9351(1 - e^{-2.1224x})$
	user 1 standing	Type 3: $3.2956(x/15.94)^{0.2733}$
Netflix in [34]	ElFuente1	Type 1: $33.4215 \ln(1 + 0.784x + 10.0826y)$
	BigBuckBunny	Type 2: $103.3464(1 - e^{-0.23166x - 2.9792y})$
	BirdsInCage	Type 3: $61.8622(x/15 + y/1.1664)^{0.5301}$

The existence of y in some expressions above can be understood that the coefficients in (35) (36) (37) depend on y . In simulations below, we fix y so that the utility function depends on only the rate.

7.3 Parameter setting

We first state settings that apply to all simulations. Based on [16], we model the path loss between each legitimate user and the Metaverse server as $128.1 + 37.6 \log(\text{distance})$ along with 8 decibels (dB) for the standard deviation of shadow fading, and the unit of *distance* is kilometer. The power spectral density of Gaussian noise σ_n^2 is -174 dBm/Hz (i.e., 4 zeptowatts/Hz, the value for thermal noise at 20 °C room temperature [36]).

In addition, some default settings are as follows, unless otherwise specified. N denoting the number of legitimate users is 30. The weight parameter c_n is set to 1 for all users (unless configured otherwise), which means the weighted sum-UEE just becomes sum-UEE by default. The default total bandwidth B_{total} is 20 MHz. The circuit power $p_n^{c_{lr}}$ is 2 dBm (i.e., 1.6 milliwatts) for each n . Both the eavesdropping rate $r_{n,e}$ and the minimum transmission rate r_n^{\min} are 20 kilobits per second (Kbps) by default. For the utility functions,

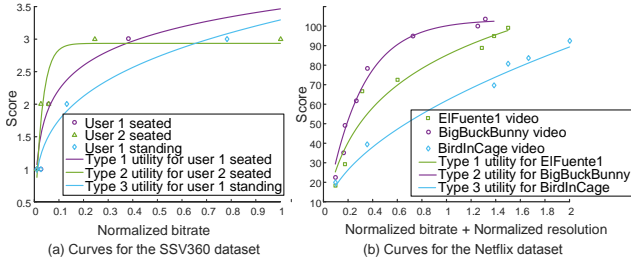


Figure 2: The curve-fitting results using Types 1, 2, and 3 utility functions. In both subfigures, the normalized video bitrate is obtained from dividing the bitrate by the maximum value of 15.94 Mbps (resp., 15 Mbps) in the SSV360 (resp., Netflix) dataset. In Fig. 2(b), the normalized resolution is the result of dividing the resolution by the maximum resolution of 1920×1080 pixels (i.e., 1080p) in the Netflix dataset.

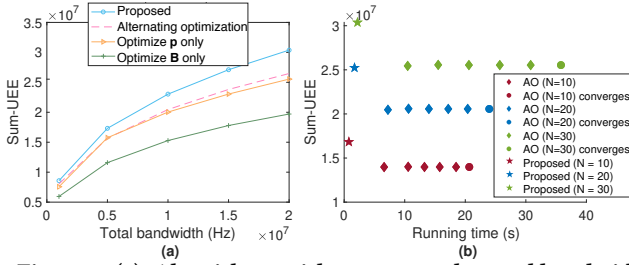


Figure 3: (a). Algorithms with respect to the total bandwidth. (b). Running time and objective-function value under each algorithm, where AO is short for alternating optimization.

we set $\kappa_n = 1$, $a_n = 0.5$, $b_n = 1$, $c_n = 0$, and $d_n = 0$ by default. In all simulations, we stop the algorithm after obtaining a 0.01-global optimum, whose meaning is discussed at the end of Section 5.2.

7.4 Comparison of different algorithms

We compare our Algorithm 1 with the following baselines:

- (i) **Optimize B only:** Here we let p_n for each n be 1 milliwatt (i.e., 10^{-3} W), which will be substituted into Problem \mathbb{P}_1 . Then “optimizing B only” becomes convex optimization, for which the KKT conditions are analyzed to obtain the solution.
- (ii) **Optimize p only:** In this case, we let B_n for each n be B_{total}/N , which will be substituted into Problem \mathbb{P}_1 . Then “optimizing p only” belongs to convex optimization, for which the KKT conditions are inspected to acquire the solution.
- (iii) **Alternating optimization:** Starting with a feasible initialization, we perform “(i)” and “(ii)” above in an alternating manner, until convergence (when the relative improvement between two consecutive iterations is negligible).

For the detailed analyses of the baseline algorithms, interested readers can refer to Appendix C.

We compare Algorithm 1 with the above baselines in Fig. 3, where Type 3 utility function is used. Fig. 3(a) plots the sum-UEE with respect to the total bandwidth B_{total} , and shows that our proposed algorithm achieves a larger sum-UEE than all the baselines. For each curve, as B_{total} increases, the sum-UEE grows but at a slower rate. Formally proving this is not in this paper’s scope, but it seems intuitive since each user’s UEE is an increasing and concave function of the bandwidth, given the transmission power.

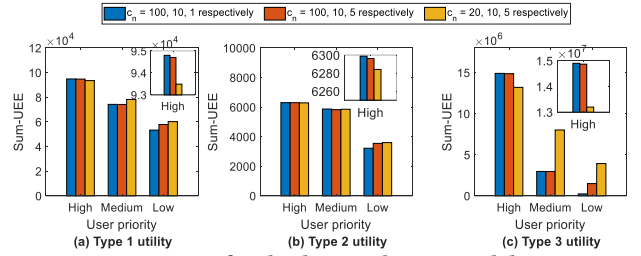


Figure 4: Sum-UEE for high-, medium-, and low-priority users, under different c_n values, for Type 1, 2, or 3 utility.

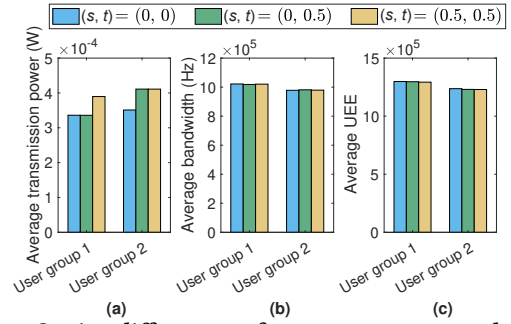


Figure 5: Setting different $r_{n,e}$ for two user groups, where the legend “ (s, t) ” means that $r_{n,e}$ for user U_n in Group 1 is set as $s \cdot r_n^{\min}$ while $r_{n,e}$ for user U_n in Group 2 equals $t \cdot r_n^{\min}$.

Fig. 3(b) displays the convergence performance of our proposed algorithm and alternating optimization (AO). Our algorithm always obtains a better sum-UEE and converges much faster. In particular, on a laptop with 8GB of RAM and 256GB of storage, the proposed algorithm converges within 3 seconds, but the AO approach takes around 20, 24, 36 seconds under $N = 10, 20, 30$, respectively.

7.5 The priority levels of users

Here we explore the influence of the priority of users under different utility functions. We consider that 30 users are evenly classified into three priority levels, corresponding to different weights c_n . Larger c_n means more weight in our studied optimization. For example, the legend “ $c_n = 100, 10, 1$ ” in Fig. 4 means that 10 users with c_n being 100 (resp., 10 and 1) have high (resp., medium and low) priority.

Fig. 4(a) (b) and (c) use utility functions of Types 1, 2, and 3, respectively. The sum-UEE of users in each priority group is plotted. In each subfigure, the bar charts show that the sum-UEE of the high-priority group is the largest, while that of the low-priority group is the lowest, matching the intuition, since higher priority means larger c_n and “more say” in the weighted sum-UEE optimization. In addition, the numbers in Fig. 4(c) for Type 3 utility $u_3 := r_{n,s}^{0.5}$ are greater than the corresponding ones in Fig. 4(a) for Type 1 utility $u_1 := \ln(1 + 0.5r_{n,s})$, which are further larger than those in Fig. 4(b) for Type 2 utility $u_2 := 1 - e^{-0.5r_{n,s}}$. The above is consistent with $u_3 > u_1 > u_2$ for large $r_{n,s}$ (in the unit of bps).

In Fig. 4’s subfigures, from Case 1 of “ $c_n = 100, 10, 1$ ” to Case 2 of “ $c_n = 100, 10, 5$ ”, and further to Case 3 of “ $c_n = 20, 10, 5$ ”, the relative dominance of high-priority group decreases while the relative weight of low-priority group increases, which accords with declining (resp., rising) sum-UEE of high-priority (resp., low-priority)

group from Case 1 to Case 2, and further to Case 3. For the medium-priority group, as expected, the sum-UEE decreases from Case 1 to Case 2 (though not clear in the plots without zooming in), and increases from Case 2 to Case 3. The above demonstrates the impact of the weight c_n as the priority level.

7.6 Impact of individual rate constraints

Now we report the effect of varying $r_{n,e}$. The number of users N is set as 20, and we divide them equally into two groups with $r_{n,e}$ as $s \cdot r_n^{\min}$ and $t \cdot r_n^{\min}$, respectively, where r_n^{\min} is the default 20 Kbps. Each group's average transmission power, average allocated bandwidth, and average UEE are plotted in Fig. 5(a), (b), and (c), respectively. Also, Fig. 5 uses Type 3 utility function and evaluates (s, t) as $(0, 0)$, $(0, 0.5)$, and $(0.5, 0.5)$, respectively. From $(0, 0)$ to $(0, 0.5)$ (resp., $(0, 0.5)$ to $(0.5, 0.5)$), the second (resp., first) group's average transmission power increases. This is intuitive since raising a group's $r_{n,e}$ with everything else unchanged requires the group to enlarge the transmission power and hence the data rate. The bandwidth allocation does not vary much under the cases of $(0, 0)$, $(0, 0.5)$, and $(0.5, 0.5)$. For each group, the average UEE slightly drops as $r_{n,e}$ grows, which seems intuitive since each user's utility $f_n(r_n(p_n, B_n) - r_{n,e})$ is negatively correlated with $r_{n,e}$.

For more simulation results (e.g., how our proposed algorithm performs when the number of users changes or when there are heterogeneous types of utility functions among the users), interested readers can refer to Appendices E.1 and E.2.

8 CONCLUSION

In this paper, in a wireless network for the Metaverse, we have studied the weighted optimization of all users' utility-energy efficiency (UEE) under physical-layer security. The formulated problem belongs to non-convex optimization, and we solve it via a transform to parametric convex optimization. The resulting algorithm is optimal in terms of both the solution quality and the order of time complexity. Simulation results are provided with utility functions validated by real data. We envision more research to adopt our transform technique due to its broad applicability to other problems in wireless networks and mobile computing.

REFERENCES

- [1] Y. Wang, Z. Su, N. Zhang, R. Xing, D. Liu, T. H. Luan, and X. Shen, "A survey on Metaverse: Fundamentals, security, and privacy," *IEEE Communications Surveys & Tutorials (COMST)*, 2022.
- [2] J.-M. Chung, "XR HMDs and detection technology," in *Emerging Metaverse XR and Video Multimedia Technologies: Modern Streaming and Multimedia Systems and Applications*, 2022, pp. 99–139.
- [3] V. Nair, G. M. Garrido, and D. Song, "Exploring the unprecedented privacy risks of the Metaverse," *arXiv preprint arXiv:2207.13176*, 2022.
- [4] M. R. Zamani, M. Eslami, M. Khorramizadeh, H. Zamani, and Z. Ding, "Optimizing weighted-sum energy efficiency in downlink and uplink NOMA systems," *IEEE Transactions on Vehicular Technology*, vol. 69, no. 10, pp. 11 112–11 127, 2020.
- [5] Q. Wu, W. Chen, D. W. K. Ng, J. Li, and R. Schober, "User-centric energy efficiency maximization for wireless powered communications," *IEEE Transactions on Wireless Communications*, vol. 15, no. 10, pp. 6898–6912, 2016.
- [6] W. Du, Z. Chu, G. Chen, P. Xiao, Z. Lin, C. Huang, and W. Hao, "Weighted sum-rate and energy efficiency maximization for joint ITS and IRS assisted multiuser MIMO networks," *IEEE Transactions on Communications*, 2022.
- [7] F. Meshkati, H. V. Poor, and S. C. Schwartz, "Energy efficiency-delay tradeoffs in CDMA networks: A game-theoretic approach," *IEEE Transactions on Information Theory*, vol. 55, no. 7, pp. 3220–3228, 2009.
- [8] X. Huang, W. Xu, H. Shen, H. Zhang, and X. You, "Utility-energy efficiency oriented user association with power control in heterogeneous networks," *IEEE Wireless Communications Letters*, vol. 7, no. 4, pp. 526–529, 2018.

- [9] Y. Jiang and Y. Zou, "Secrecy energy efficiency maximization for multi-user multi-eavesdropper cell-free massive MIMO networks," *IEEE Transactions on Vehicular Technology*, 2023.
- [10] A. Zappone, P.-H. Lin, and E. A. Jorswieck, "Secrecy energy efficiency for MIMO single-and multi-cell downlink transmission with confidential messages," *IEEE Transactions on Information Forensics and Security*, 2019.
- [11] W. Yu, T. J. Chua, and J. Zhao, "Asynchronous hybrid reinforcement learning for latency and reliability optimization in the Metaverse over wireless communications," *IEEE Journal on Selected Areas in Communications (JSAC)*, 2023. [Online]. Available: <https://arxiv.org/abs/2212.14749>
- [12] Z. Meng, C. She, G. Zhao, and D. De Martini, "Sampling, communication, and prediction co-design for synchronizing the real-world device and digital model in Metaverse," *IEEE Journal on Selected Areas in Communications (JSAC)*, 2022.
- [13] J. Wang, H. Du, Z. Tian, D. Niyato, J. Kang, and X. Shen, "Semantic-aware sensing information transmission for Metaverse: A contest theoretic approach," *IEEE Transactions on Wireless Communications (TWC)*, 2023.
- [14] Y. Jiang, J. Kang, D. Niyato, X. Ge, Z. Xiong, C. Miao, and X. Shen, "Reliable distributed computing for Metaverse: A hierarchical game-theoretic approach," *IEEE Transactions on Vehicular Technology (TVT)*, 2022.
- [15] Y. Ren, R. Xie, F. R. Yu, T. Huang, and Y. Liu, "Quantum collective learning and many-to-many matching game in the Metaverse for connected and autonomous vehicles," *IEEE Transactions on Vehicular Technology (TVT)*, 2022.
- [16] X. Zhou, C. Liu, and J. Zhao, "Resource allocation of federated learning for the Metaverse with mobile augmented reality," *submitted to IEEE Transactions on Wireless Communications (Major Revision)*, 2023. <https://arxiv.org/abs/2211.08705>
- [17] J. Xu and R. Zhang, "Throughput optimal policies for energy harvesting wireless transmitters with non-ideal circuit power," *IEEE Journal on Selected Areas in Communications*, vol. 32, no. 2, pp. 322–332, 2013.
- [18] Y. Jiang, Y. Zou, J. Ouyang, and J. Zhu, "Secrecy energy efficiency optimization for artificial noise aided physical-layer security in OFDM-based cognitive radio networks," *IEEE Transactions on Vehicular Technology*, 2018.
- [19] A. Cambini and L. Martein, *Generalized Convexity and Optimization: Theory and Applications*. Springer Science & Business Media, 2008, vol. 616.
- [20] S. Boyd and L. Vandenberghe, *Convex Optimization*. Cambridge Univ Press, 2004.
- [21] D. Yang, G. Xue, X. Fang, and J. Tang, "Crowdsourcing to smartphones: Incentive mechanism design for mobile phone sensing," in *ACM MobiCom*, 2012.
- [22] Q. Liu, S. Huang, J. Opadere, and T. Han, "An edge network orchestrator for mobile augmented reality," in *IEEE INFOCOM*, 2018, pp. 756–764.
- [23] J. Mo and J. Walrand, "Fair end-to-end window-based congestion control," *IEEE/ACM Transactions on Networking*, vol. 8, no. 5, pp. 556–567, 2000.
- [24] Z. Xiong, J. Zhao, D. Niyato, R. Deng, and J. Zhang, "Reward optimization for content providers with mobile data subsidization: A hierarchical game approach," *IEEE Transactions on Network Science and Engineering*, 2020.
- [25] Y. Jong, "An efficient global optimization algorithm for nonlinear sum-of-ratios problem," *Optimization Online*, pp. 1–21, 2012.
- [26] K. Shen and W. Yu, "Fractional programming for communication systems-Part I: Power control and beamforming," *IEEE Transactions on Signal Processing*, 2018.
- [27] —, "Fractional programming for communication systems-Part II: Uplink scheduling via matching," *IEEE Transactions on Signal Processing*, 2018.
- [28] A. Cambini, L. Martein, and S. Schaible, "On the pseudoconvexity of the sum of two linear fractional functions," in *7th International Symposium on Generalized Convexity and Generalized Monotonicity*, 2005, pp. 161–172.
- [29] J. Zhao, X. Zhou, Y. Li, and L. Qian, "Optimizing utility-energy efficiency for the Metaverse over wireless networks under physical layer security," 2023, the full version of the submitted paper, which is uploaded to arXiv before the paper deadline and available at <https://arxiv.org/pdf/2303.04683.pdf>
- [30] L. P. Qian, Y. J. Zhang, and J. Huang, "MAPEL: Achieving global optimality for a non-convex wireless power control problem," *IEEE Transactions on Wireless Communications*, vol. 8, no. 3, pp. 1553–1563, 2009.
- [31] M. Zhao, J.-J. Yu, W.-T. Li, D. Liu, S. Yao, W. Feng, C. She, and T. Q. Quek, "Energy-aware task offloading and resource allocation for time-sensitive services in mobile edge computing systems," *IEEE Transactions on Vehicular Technology*, 2021.
- [32] W. da Cruz Vieira, A. Bucci, and S. Marsiglio, "Welfare and convergence speed in the Ramsey model under two classes of Gorman preferences," *Italian Economic Journal*, vol. 7, no. 1, pp. 37–58, 2021.
- [33] M. Elwardy, H.-J. Zepernick, and Y. Hu, "SSV360: A dataset on subjective quality assessment of 360° videos for standing and seated viewing on an HMD," in *IEEE Conference on Virtual Reality and 3D User Interfaces*, 2022.
- [34] <https://github.com/Netflix/vmaf/blob/master/resource/doc/datasets.md>
- [35] J. Gutiérrez and K. Brunnström, "VQEG column: Recent contributions to ITU recommendations," *ACM SIGMultimedia Records*, vol. 12, no. 3, pp. 1–1, 2022.
- [36] X. Huang, G. Dolmans, H. de Groot, and J. R. Long, "Noise and sensitivity in RF envelope detection receivers," *IEEE Transactions on Circuits and Systems II: Express Briefs*, vol. 60, no. 10, pp. 637–641, 2013.
- [37] V. I. Ivanov, "Characterization of radially lower semicontinuous pseudoconvex functions," *Journal of Optimization Theory and Applications*, vol. 184, no. 2, pp. 368–383, 2020.

Appendices:

We introduce some notation to be used in the appendices. For a scalar function $f(x_1, x_2, \dots, x_M)$ of M variables x_1, x_2, \dots, x_M , we use $\nabla_{x_m} f(x_1, x_2, \dots, x_M)$ where $m \in \{1, 2, \dots, M\}$ to denote the partial derivative of $f(x_1, x_2, \dots, x_M)$ with respect to x_m , and use $\nabla_{x_m} f(x_1, x_2, \dots, x_M)|_{x_m=x_m^*}$ to denote the corresponding result when x_m equals a given value x_m^* . For a K -element set $\{x_{i_1}, x_{i_2}, \dots, x_{i_K}\}$ of variables, which is a subset of $\{x_1, x_2, \dots, x_M\}$, we define $\nabla_{x_{i_1}, x_{i_2}, \dots, x_{i_K}} f(x_1, x_2, \dots, x_M)$ as the vector $[\nabla_{x_{i_k}} f(x_1, x_2, \dots, x_M)]_{k=1,2,\dots,K}$.

A EXPLAINING (29)

To establish (29), we will prove $(\partial\phi_{1,n}(\boldsymbol{\beta}, \boldsymbol{\nu})) / (\partial\beta_n)$ and $(\partial\phi_{2,n}(\boldsymbol{\beta}, \boldsymbol{\nu})) / (\partial\nu_n)$ equal $p_n^\#(\boldsymbol{\beta}, \boldsymbol{\nu}) + p_n^{\text{cir}}$. (A.1)

The definitions of $\phi_{1,n}(\boldsymbol{\beta}, \boldsymbol{\nu})$ and $\phi_{2,n}(\boldsymbol{\beta}, \boldsymbol{\nu})$ in (20) and (21) use $[\mathbf{p}^\#(\boldsymbol{\beta}, \boldsymbol{\nu}), \mathbf{B}^\#(\boldsymbol{\beta}, \boldsymbol{\nu})]$, which denotes a globally optimal solution to $\mathbb{P}_3(\boldsymbol{\beta}, \boldsymbol{\nu})$. Hence, below we analyze $\mathbb{P}_3(\boldsymbol{\beta}, \boldsymbol{\nu})$.

Problem $\mathbb{P}_3(\boldsymbol{\beta}, \boldsymbol{\nu})$ belongs to convex optimization and Slater's condition holds, as shown in the proof of Lemma 5.1. Then the Karush–Kuhn–Tucker (KKT) conditions are necessary and sufficient to obtain the globally optimal solution, as stated in Lemma 4.3. To this end, we define the Lagrange function:

$$L_{\mathbb{P}_3}(\mathbf{p}, \mathbf{B}, \boldsymbol{\tau}, \lambda \mid \boldsymbol{\beta}, \boldsymbol{\nu}) = -\sum_{n \in \mathcal{N}} \mathcal{F}_n(p_n, B_n \mid \beta_n, \nu_n) + \sum_{n \in \mathcal{N}} \tau_n \cdot (r_n^{\min} - r_n) + \lambda \cdot (\sum_{n \in \mathcal{N}} B_n - B_{\text{total}}), \quad (\text{A.2})$$

where $\boldsymbol{\tau}$ and λ are called Lagrange multipliers.

The KKT conditions of Problem $\mathbb{P}_3(\boldsymbol{\beta}, \boldsymbol{\nu})$ are as follows, with $L_{\mathbb{P}_3}$ short for $L_{\mathbb{P}_3}(\mathbf{p}, \mathbf{B}, \boldsymbol{\tau}, \lambda \mid \boldsymbol{\beta}, \boldsymbol{\nu})$:

Stationarity:

$$\frac{\partial L_{\mathbb{P}_3}}{\partial p_n} = 0, \text{ for all } n \in \mathcal{N}, \quad (\text{A.3a})$$

$$\frac{\partial L_{\mathbb{P}_3}}{\partial B_n} = 0, \text{ for all } n \in \mathcal{N}, \quad (\text{A.3b})$$

Complementary slackness:

$$\tau_n \cdot (r_n^{\min} - r_n(p_n, B_n)) = 0, \text{ for all } n \in \mathcal{N}, \quad (\text{A.3c})$$

$$\lambda \cdot (\sum_{n \in \mathcal{N}} B_n - B_{\text{total}}) = 0; \quad (\text{A.3d})$$

Primal feasibility:

$$r_n(p_n, B_n) \geq r_n^{\min}, \text{ for all } n \in \mathcal{N}, \quad (\text{A.3e})$$

$$\sum_{n \in \mathcal{N}} B_n \leq B_{\text{total}}; \quad (\text{A.3f})$$

Dual feasibility:

$$\tau_n \geq 0, \text{ for all } n \in \mathcal{N}. \quad (\text{A.3g})$$

$$\lambda \geq 0. \quad (\text{A.3h})$$

Recall that we use $[\mathbf{p}^\#(\boldsymbol{\beta}, \boldsymbol{\nu}), \mathbf{B}^\#(\boldsymbol{\beta}, \boldsymbol{\nu})]$ to denote a globally optimal solution to $\mathbb{P}_3(\boldsymbol{\beta}, \boldsymbol{\nu})$, where $\mathbf{p}^\#(\boldsymbol{\beta}, \boldsymbol{\nu}) = [p_n^\#(\boldsymbol{\beta}, \boldsymbol{\nu})]_{n \in \mathcal{N}}$ and $\mathbf{B}^\#(\boldsymbol{\beta}, \boldsymbol{\nu}) = [B_n^\#(\boldsymbol{\beta}, \boldsymbol{\nu})]_{n \in \mathcal{N}}$. Hence, $[\mathbf{p}^\#(\boldsymbol{\beta}, \boldsymbol{\nu}), \mathbf{B}^\#(\boldsymbol{\beta}, \boldsymbol{\nu})]$ satisfies the KKT conditions above. Using (A.2) (A.3c) and (A.3d), we know

$$\begin{aligned} L_{\mathbb{P}_3}(\mathbf{p}^\#(\boldsymbol{\beta}, \boldsymbol{\nu}), \mathbf{B}^\#(\boldsymbol{\beta}, \boldsymbol{\nu}), \boldsymbol{\tau}, \lambda \mid \boldsymbol{\beta}, \boldsymbol{\nu}) &= -\sum_{n \in \mathcal{N}} \mathcal{F}_n(p_n^\#(\boldsymbol{\beta}, \boldsymbol{\nu}), B_n^\#(\boldsymbol{\beta}, \boldsymbol{\nu}) \mid \beta_n, \nu_n) \\ &+ \sum_{n \in \mathcal{N}} \tau_n \cdot (r_n^{\min} - r_n(p_n^\#(\boldsymbol{\beta}, \boldsymbol{\nu}), B_n^\#(\boldsymbol{\beta}, \boldsymbol{\nu}))) \\ &+ \lambda \cdot (\sum_{n \in \mathcal{N}} B_n^\#(\boldsymbol{\beta}, \boldsymbol{\nu}) - B_{\text{total}}) \\ &= -\sum_{n \in \mathcal{N}} \mathcal{F}_n(p_n^\#(\boldsymbol{\beta}, \boldsymbol{\nu}), B_n^\#(\boldsymbol{\beta}, \boldsymbol{\nu}) \mid \beta_n, \nu_n). \end{aligned} \quad (\text{A.4})$$

For notation simplicity, we group $\boldsymbol{\beta}$ and $\boldsymbol{\nu}$ together to define $\boldsymbol{\alpha}$; i.e., $\boldsymbol{\alpha} := [\boldsymbol{\beta}, \boldsymbol{\nu}]$. Note that (A.4) above holds for any $\boldsymbol{\alpha}$. Hence, it holds that

$$\begin{aligned} \nabla_{\boldsymbol{\alpha}} (\sum_{n \in \mathcal{N}} \mathcal{F}_n(p_n^\#(\boldsymbol{\beta}, \boldsymbol{\nu}), B_n^\#(\boldsymbol{\beta}, \boldsymbol{\nu}) \mid \beta_n, \nu_n)) &= -\nabla_{\boldsymbol{\alpha}} (L_{\mathbb{P}_3}(\mathbf{p}^\#(\boldsymbol{\beta}, \boldsymbol{\nu}), \mathbf{B}^\#(\boldsymbol{\beta}, \boldsymbol{\nu}), \boldsymbol{\tau}, \lambda \mid \boldsymbol{\beta}, \boldsymbol{\nu})). \end{aligned} \quad (\text{A.5})$$

Based on (A.5), to get $\nabla_{\boldsymbol{\alpha}} (\sum_{n \in \mathcal{N}} \mathcal{F}_n(p_n^\#(\boldsymbol{\beta}, \boldsymbol{\nu}), B_n^\#(\boldsymbol{\beta}, \boldsymbol{\nu}) \mid \beta_n, \nu_n))$, we compute $\nabla_{\boldsymbol{\alpha}} (L_{\mathbb{P}_3}(\mathbf{p}^\#(\boldsymbol{\beta}, \boldsymbol{\nu}), \mathbf{B}^\#(\boldsymbol{\beta}, \boldsymbol{\nu}), \boldsymbol{\tau}, \lambda \mid \boldsymbol{\beta}, \boldsymbol{\nu}))$ and take its negative. We have

$$\begin{aligned} \nabla_{\boldsymbol{\alpha}} (L_{\mathbb{P}_3}(\mathbf{p}^\#(\boldsymbol{\beta}, \boldsymbol{\nu}), \mathbf{B}^\#(\boldsymbol{\beta}, \boldsymbol{\nu}), \boldsymbol{\tau}, \lambda \mid \boldsymbol{\beta}, \boldsymbol{\nu})) &= \sum_{n \in \mathcal{N}} \left\{ \left[\begin{array}{c} (\nabla_{p_n} L_{\mathbb{P}_3}(\mathbf{p}, \mathbf{B}, \boldsymbol{\tau}, \lambda \mid \boldsymbol{\beta}, \boldsymbol{\nu}))|_{\substack{p=p^\#(\boldsymbol{\beta}, \boldsymbol{\nu}) \\ b=b^\#(\boldsymbol{\beta}, \boldsymbol{\nu})}} \\ \nabla_{\boldsymbol{\alpha}} p_n^\#(\boldsymbol{\beta}, \boldsymbol{\nu}) \end{array} \right] \right. \\ &+ \sum_{n \in \mathcal{N}} \left\{ \left[\begin{array}{c} (\nabla_{B_n} L_{\mathbb{P}_3}(\mathbf{p}, \mathbf{B}, \boldsymbol{\tau}, \lambda \mid \boldsymbol{\beta}, \boldsymbol{\nu}))|_{\substack{p=p^\#(\boldsymbol{\beta}, \boldsymbol{\nu}) \\ b=b^\#(\boldsymbol{\beta}, \boldsymbol{\nu})}} \\ \nabla_{\boldsymbol{\alpha}} B_n^\#(\boldsymbol{\beta}, \boldsymbol{\nu}) \end{array} \right] \right. \\ &+ \left. \left[\begin{array}{c} (\nabla_{\boldsymbol{\alpha}} L_{\mathbb{P}_3}(\mathbf{p}, \mathbf{B}, \boldsymbol{\tau}, \lambda \mid \boldsymbol{\beta}, \boldsymbol{\nu}))|_{\substack{p=p^\#(\boldsymbol{\beta}, \boldsymbol{\nu}) \\ b=b^\#(\boldsymbol{\beta}, \boldsymbol{\nu})}} \end{array} \right] \right\}. \end{aligned} \quad (\text{A.6})$$

From (A.3a) and (A.3b), we have

$$\begin{aligned} (\nabla_{p_n} L_{\mathbb{P}_3}(\mathbf{p}, \mathbf{B}, \boldsymbol{\tau}, \lambda \mid \boldsymbol{\beta}, \boldsymbol{\nu}))|_{\substack{p=p^\#(\boldsymbol{\beta}, \boldsymbol{\nu}) \\ b=b^\#(\boldsymbol{\beta}, \boldsymbol{\nu})}} &= 0, \text{ and} \\ \nabla_{B_n} L_{\mathbb{P}_3}(\mathbf{p}, \mathbf{B}, \boldsymbol{\tau}, \lambda \mid \boldsymbol{\beta}, \boldsymbol{\nu})|_{\substack{p=p^\#(\boldsymbol{\beta}, \boldsymbol{\nu}) \\ b=b^\#(\boldsymbol{\beta}, \boldsymbol{\nu})}} &= 0, \end{aligned}$$

which are used in (A.6) to obtain

$$\begin{aligned} \nabla_{\boldsymbol{\alpha}} (L_{\mathbb{P}_3}(\mathbf{p}^\#(\boldsymbol{\beta}, \boldsymbol{\nu}), \mathbf{B}^\#(\boldsymbol{\beta}, \boldsymbol{\nu}), \boldsymbol{\tau}, \lambda \mid \boldsymbol{\beta}, \boldsymbol{\nu})) &= \left[\begin{array}{c} (\nabla_{\boldsymbol{\alpha}} L_{\mathbb{P}_3}(\mathbf{p}, \mathbf{B}, \boldsymbol{\tau}, \lambda \mid \boldsymbol{\beta}, \boldsymbol{\nu}))|_{\substack{p=p^\#(\boldsymbol{\beta}, \boldsymbol{\nu}) \\ b=b^\#(\boldsymbol{\beta}, \boldsymbol{\nu})}} \end{array} \right]. \end{aligned} \quad (\text{A.7})$$

From (A.2) (A.5) and (A.7), it holds that

$$\begin{aligned} \nabla_{\boldsymbol{\alpha}} (\sum_{n \in \mathcal{N}} \mathcal{F}_n(p_n^\#(\boldsymbol{\beta}, \boldsymbol{\nu}), B_n^\#(\boldsymbol{\beta}, \boldsymbol{\nu}) \mid \beta_n, \nu_n)) &= - \left[\begin{array}{c} (\nabla_{\boldsymbol{\alpha}} L_{\mathbb{P}_3}(\mathbf{p}, \mathbf{B}, \boldsymbol{\tau}, \lambda \mid \boldsymbol{\beta}, \boldsymbol{\nu}))|_{\substack{p=p^\#(\boldsymbol{\beta}, \boldsymbol{\nu}) \\ b=b^\#(\boldsymbol{\beta}, \boldsymbol{\nu})}} \end{array} \right] \\ &= \sum_{n \in \mathcal{N}} \left[\begin{array}{c} (\nabla_{\boldsymbol{\alpha}} \mathcal{F}_n(p_n, B_n \mid \beta_n, \nu_n))|_{\substack{p=p^\#(\boldsymbol{\beta}, \boldsymbol{\nu}) \\ b=b^\#(\boldsymbol{\beta}, \boldsymbol{\nu})}} \end{array} \right]. \end{aligned} \quad (\text{A.8})$$

Using the above and (16), we further acquire

$$\begin{aligned} \nabla_{\beta_n} (\sum_{n \in \mathcal{N}} \mathcal{F}_n(p_n^\#(\boldsymbol{\beta}, \boldsymbol{\nu}), B_n^\#(\boldsymbol{\beta}, \boldsymbol{\nu}) \mid \beta_n, \nu_n)) &= \sum_{n \in \mathcal{N}} \left[\begin{array}{c} (\nabla_{\beta_n} \mathcal{F}_n(p_n, B_n \mid \beta_n, \nu_n))|_{\substack{p=p^\#(\boldsymbol{\beta}, \boldsymbol{\nu}) \\ b=b^\#(\boldsymbol{\beta}, \boldsymbol{\nu})}} \end{array} \right] \\ &= -\sum_{n \in \mathcal{N}} [v_n \cdot (p_n^\#(\boldsymbol{\beta}, \boldsymbol{\nu}) + p_n^{\text{cir}})], \end{aligned} \quad (\text{A.9})$$

and

$$\begin{aligned} \nabla_{\nu_n} (\sum_{n \in \mathcal{N}} \mathcal{F}_n(p_n^\#(\boldsymbol{\beta}, \boldsymbol{\nu}), B_n^\#(\boldsymbol{\beta}, \boldsymbol{\nu}) \mid \beta_n, \nu_n)) &= \sum_{n \in \mathcal{N}} \left[\begin{array}{c} (\nabla_{\nu_n} \mathcal{F}_n(p_n, B_n \mid \beta_n, \nu_n))|_{\substack{p=p^\#(\boldsymbol{\beta}, \boldsymbol{\nu}) \\ b=b^\#(\boldsymbol{\beta}, \boldsymbol{\nu})}} \end{array} \right] \\ &= \sum_{n \in \mathcal{N}} [F_n(p_n^\#(\boldsymbol{\beta}, \boldsymbol{\nu}), B_n^\#(\boldsymbol{\beta}, \boldsymbol{\nu})) - \beta_n \cdot (p_n^\#(\boldsymbol{\beta}, \boldsymbol{\nu}) + p_n^{\text{cir}})]. \end{aligned} \quad (\text{A.10})$$

Since (A.9) and (A.10) hold for any $\boldsymbol{\beta}$ and $\boldsymbol{\nu}$, we obtain

$$\begin{aligned} \nabla_{\beta_n} \mathcal{F}_n(p_n^\#(\boldsymbol{\beta}, \boldsymbol{\nu}), B_n^\#(\boldsymbol{\beta}, \boldsymbol{\nu}) \mid \beta_n, \nu_n) &= - [v_n \cdot (p_n^\#(\boldsymbol{\beta}, \boldsymbol{\nu}) + p_n^{\text{cir}})], \end{aligned} \quad (\text{A.11})$$

and

$$\begin{aligned} & \nabla_{v_n} \mathcal{F}_n(p_n^\#(\boldsymbol{\beta}, \boldsymbol{\nu}), B_n^\#(\boldsymbol{\beta}, \boldsymbol{\nu}) | \beta_n, v_n) \\ &= [F_n(p_n^\#(\boldsymbol{\beta}, \boldsymbol{\nu}), B_n^\#(\boldsymbol{\beta}, \boldsymbol{\nu})) - \beta_n \cdot (p_n^\#(\boldsymbol{\beta}, \boldsymbol{\nu}) + p_n^{\text{cir}})]. \end{aligned} \quad (\text{A.12})$$

From the definition of $\mathcal{F}_n(p_n, B_n | \beta_n, v_n)$ in (16), we also have

$$\begin{aligned} & \nabla_{\beta_n} \mathcal{F}_n(p_n^\#(\boldsymbol{\beta}, \boldsymbol{\nu}), B_n^\#(\boldsymbol{\beta}, \boldsymbol{\nu}) | \beta_n, v_n) \\ &= v_n \cdot [\nabla_{p_n} F_n(p_n, B_n) |_{p_n=p_n^\#(\boldsymbol{\beta}, \boldsymbol{\nu})} \cdot \nabla_{\beta_n} p_n^\#(\boldsymbol{\beta}, \boldsymbol{\nu}) \\ &+ \nabla_{B_n} F_n(p_n, B_n) |_{B_n=B_n^\#(\boldsymbol{\beta}, \boldsymbol{\nu})} \cdot \nabla_{\beta_n} B_n^\#(\boldsymbol{\beta}, \boldsymbol{\nu}) - (p_n^\#(\boldsymbol{\beta}, \boldsymbol{\nu}) + p_n^{\text{cir}})], \end{aligned} \quad (\text{A.13})$$

and

$$\begin{aligned} & \nabla_{v_n} \mathcal{F}_n(p_n^\#(\boldsymbol{\beta}, \boldsymbol{\nu}), B_n^\#(\boldsymbol{\beta}, \boldsymbol{\nu}) | \beta_n, v_n) \\ &= [F_n(p_n^\#(\boldsymbol{\beta}, \boldsymbol{\nu}), B_n^\#(\boldsymbol{\beta}, \boldsymbol{\nu})) - \beta_n \cdot (p_n^\#(\boldsymbol{\beta}, \boldsymbol{\nu}) + p_n^{\text{cir}})] \\ &+ v_n \cdot [\nabla_{p_n} F_n(p_n, B_n) |_{p_n=p_n^\#(\boldsymbol{\beta}, \boldsymbol{\nu})} \cdot \nabla_{v_n} p_n^\#(\boldsymbol{\beta}, \boldsymbol{\nu}) \\ &+ \nabla_{B_n} F_n(p_n, B_n) |_{B_n=B_n^\#(\boldsymbol{\beta}, \boldsymbol{\nu})} \cdot \nabla_{v_n} B_n^\#(\boldsymbol{\beta}, \boldsymbol{\nu}) \\ &- \beta_n \cdot \nabla_{v_n} p_n^\#(\boldsymbol{\beta}, \boldsymbol{\nu})]. \end{aligned} \quad (\text{A.14})$$

Comparing (A.11) and (A.13), and comparing (A.12) and (A.14), since we always enforce $v_n > 0$, we have proved

$$\begin{aligned} & [\nabla_{p_n} F_n(p_n, B_n) |_{p_n=p_n^\#(\boldsymbol{\beta}, \boldsymbol{\nu})} \cdot \nabla_{\beta_n} p_n^\#(\boldsymbol{\beta}, \boldsymbol{\nu}) \\ &+ \nabla_{B_n} F_n(p_n, B_n) |_{B_n=B_n^\#(\boldsymbol{\beta}, \boldsymbol{\nu})} \cdot \nabla_{\beta_n} B_n^\#(\boldsymbol{\beta}, \boldsymbol{\nu})] = 0, \end{aligned} \quad (\text{A.15})$$

and

$$\begin{aligned} & [\nabla_{p_n} F_n(p_n, B_n) |_{p_n=p_n^\#(\boldsymbol{\beta}, \boldsymbol{\nu})} \cdot \nabla_{v_n} p_n^\#(\boldsymbol{\beta}, \boldsymbol{\nu}) \\ &+ \nabla_{B_n} F_n(p_n, B_n) |_{B_n=B_n^\#(\boldsymbol{\beta}, \boldsymbol{\nu})} \cdot \nabla_{v_n} B_n^\#(\boldsymbol{\beta}, \boldsymbol{\nu}) - \beta_n \cdot \nabla_{v_n} p_n^\#(\boldsymbol{\beta}, \boldsymbol{\nu})] = 0. \end{aligned} \quad (\text{A.16})$$

Based on the above, and the definitions of $\phi_{1,n}(\boldsymbol{\beta}, \boldsymbol{\nu})$ and $\phi_{2,n}(\boldsymbol{\beta}, \boldsymbol{\nu})$ in (20) and (21), the desired result (A.1) is proved.

B SOLVING PROBLEM $\mathbb{P}_3(\boldsymbol{\beta}, \boldsymbol{\nu})$

We will prove Theorem 2 and use it to solve Problem $\mathbb{P}_3(\boldsymbol{\beta}, \boldsymbol{\nu})$.

B.1 Proof of Theorem 2 which characterizes the solution to Problem $\mathbb{P}_3(\boldsymbol{\beta}, \boldsymbol{\nu})$

Some texts below are repeated from Appendix A. Problem $\mathbb{P}_3(\boldsymbol{\beta}, \boldsymbol{\nu})$ belongs to convex optimization and Slater's condition holds, as shown in the proof of Lemma 5.1. Then the Karush–Kuhn–Tucker (KKT) conditions are necessary and sufficient to obtain the globally optimal solution, as stated in Lemma 4.3.

Let $[\boldsymbol{p}^\#, \boldsymbol{B}^\#, \boldsymbol{\tau}^\#, \boldsymbol{\lambda}^\#]$ satisfy the KKT conditions of Problem $\mathbb{P}_3(\boldsymbol{\beta}, \boldsymbol{\nu})$. Then, after defining

$$\vartheta_n^\# := \frac{g_n p_n^\#}{\sigma_n^2 B_n^\#}, \quad (\text{A.17})$$

we obtain the following KKT conditions:

$$\begin{aligned} \frac{\partial L_{\mathbb{P}_3}}{\partial p_n} &= -(v_n c_n f'_n(r_{n,s}(p_n^\#, B_n^\#)) + \tau_n^\#) \frac{g_n}{\sigma_n^2 (1 + \vartheta_n^\#) \ln 2} \\ &+ v_n \beta_n = 0, \quad \forall n \in \mathcal{N}, \end{aligned} \quad (\text{A.18})$$

$$\begin{aligned} \frac{\partial L_{\mathbb{P}_3}}{\partial B_n} &= -\nabla_{B_n} \mathcal{F}_n(p_n, B_n | \beta_n, v_n) |_{B_n=B_n^\#, p_n=p_n^\#} \\ &- \tau_n^\# \nabla_{B_n} r_n(p_n, B_n) |_{B_n=B_n^\#, p_n=p_n^\#} + \lambda^\# \end{aligned} \quad (\text{A.19})$$

$$\begin{aligned} &= -\left(v_n c_n f'_n(r_{n,s}(p_n^\#, B_n^\#)) + \tau_n^\# \right) \left(\log_2(1 + \vartheta_n^\#) \right. \\ &\left. - \frac{\vartheta_n^\#}{(1 + \vartheta_n^\#) \ln 2} \right) + \lambda^\# = 0, \quad \forall n \in \mathcal{N}, \end{aligned} \quad (\text{A.20})$$

$$\lambda^\# \cdot (\sum_{n \in \mathcal{N}} B_n^\# - B_{\text{total}}) = 0, \quad (\text{A.21})$$

$$\tau_n^\# \cdot (r_n^{\min} - r_n(p_n^\#, B_n^\#)) = 0, \quad \forall n \in \mathcal{N}, \quad (\text{A.22})$$

where (A.18) and (A.20) refer to the stationarity conditions, while (A.21) and (A.22) are called complementary slackness. We show the intermediate step (A.19) since it will be useful later. For the conditions of primal feasibility (i.e., (4a) and (4b) for $[\boldsymbol{p}^\#, \boldsymbol{B}^\#]$) and dual feasibility (i.e., $\tau_n^\# \geq 0$ for all $n \in \mathcal{N}$ and $\lambda^\# \geq 0$), we will write them out at the places where we need them.

Next, we aim to simplify (A.18)-(A.22) step-by-step to obtain $[\boldsymbol{p}^\#, \boldsymbol{B}^\#, \boldsymbol{\tau}^\#, \boldsymbol{\lambda}^\#]$. To begin with, Condition 2 on Page 4 ensures $f'_n(r_{n,s}(p_n^\#, B_n^\#)) > 0$. Using this along with $\tau_n^\# \geq 0$ and $\log_2(1 + \vartheta_n^\#) - \frac{\vartheta_n^\#}{(1 + \vartheta_n^\#) \ln 2} > 0$ in (A.20), we know $\lambda^\# > 0$ so that (A.21) becomes

$$\sum_{n \in \mathcal{N}} B_n^\# = B_{\text{total}}. \quad (\text{A.23})$$

We note that both (A.18) and (A.20) have the term $v_n c_n f'_n(r_{n,s}(p_n^\#, B_n^\#)) + \tau_n^\#$, which is strictly positive due to $\tau_n^\# \geq 0$ and $f'_n(r_{n,s}(p_n^\#, B_n^\#)) > 0$ explained above. Thus, from (A.18) and (A.20), we get

$$\frac{\left(\log_2(1 + \vartheta_n^\#) - \frac{\vartheta_n^\#}{(1 + \vartheta_n^\#) \ln 2} \right) v_n}{\frac{g_n}{\sigma_n^2 (1 + \vartheta_n^\#) \ln 2}} = \frac{\lambda^\#}{\beta_n}. \quad (\text{A.24})$$

From the above equation (A.24), we solve $\vartheta_n^\#$ given $\lambda^\#$. Denoting the solution as $\psi_n(\lambda)$ to highlight its dependence on λ , we have:

$$\vartheta_n^\# = \psi_n(\lambda^\#), \text{ for } \psi_n(\lambda) := \exp\left\{1 + W\left(\frac{1}{v_n \beta_n \sigma_n^2} - 1\right)\right\} - 1. \quad (\text{A.25})$$

Once we have $\lambda^\#$, (A.17) and (A.25) mean that $\vartheta_n^\#$ denoting $\frac{g_n p_n^\#}{\sigma_n^2 B_n^\#}$ is decided. To derive $p_n^\#$ and $B_n^\#$ given $\lambda^\#$, we need another condition of $p_n^\#$ and $B_n^\#$. To this end, we notice (A.20), but (A.20) involves $\tau_n^\# \geq 0$. If $\tau_n^\# = 0$, then (A.20) together with (A.25) will decide $p_n^\#$ and $B_n^\#$ given $\lambda^\#$. Therefore, we will discuss **Case 1**: $\tau_n^\# = 0$ and **Case 2**: $\tau_n^\# > 0$ respectively for each $n \in \mathcal{N}$. From the above explanation, we first try to express $p_n^\#$ and $B_n^\#$ as expressions of $\lambda^\#$, and then substitute these expressions into our conditions to obtain $\lambda^\#$.

Before elaborating on the two cases, we note (A.19) and define a function $\gamma_n(\lambda)$ which will facilitate discussing the two cases. Specifically, given λ , then under the constraint of

$$\frac{g_n p_n}{\sigma_n^2 B_n} = \psi_n(\lambda), \text{ for } \psi_n(\lambda) \text{ defined in (A.25),} \quad (\text{A.26})$$

we define $\gamma_n(\lambda)$ as the result of $r_n(p_n, B_n) \geq r_{n,e}$ to ensure (we will discuss soon when such $r_n(p_n, B_n)$ does not exist)

$$\nabla_{B_n} \mathcal{F}_n(p_n, B_n | \beta_n, v_n) = \lambda. \quad (\text{A.27})$$

From $r_n(p_n, B_n) = B_n \log_2(1 + \frac{g_n p_n}{\sigma_n^2 B_n})$, B_n ensuring (A.26) and (A.27) is given by

$$\frac{\gamma_n(\lambda)}{\log_2(1 + \psi_n(\lambda))}. \quad (\text{A.28})$$

We aim to obtain the expression of $\gamma_n(\lambda)$ for $r_n(p_n, B_n)$ from (A.26) and (A.27). From (16) and (A.27),

$$\begin{aligned} & f'_n(r_n(p_n, B_n) - r_{n,e}) \\ &= \frac{\lambda}{v_n c_n \cdot (\log_2(1 + \psi_n(\lambda)) - \frac{\psi_n(\lambda)}{(1 + \psi_n(\lambda)) \ln 2})} = \frac{\beta_n \sigma_n^2 (1 + \psi_n(\lambda)) \ln 2}{c_n g_n}, \end{aligned} \quad (\text{A.29})$$

where the last step uses $\frac{(\log_2(1 + \psi_n(\lambda)) - \frac{\psi_n(\lambda)}{(1 + \psi_n(\lambda)) \ln 2}) v_n}{\frac{g_n}{\sigma_n^2 (1 + \psi_n(\lambda)) \ln 2}} = \frac{\lambda}{\beta_n}$ from (A.24) and (A.25).

⁵Using $r_n(p_n^\#, B_n^\#) \geq r_n^{\min}$ from (4b) and $r_n^{\min} > 0$ from Condition 1 on Page 3, we have $r_n(p_n^\#, B_n^\#) > 0$ which implies $p_n^\# > 0$ and $B_n^\# > 0$, inducing $\vartheta_n^\# > 0$. For any $x > 0$, we can prove $\log_2(1 + x) - \frac{x}{(1+x) \ln 2} > 0$, so that $\log_2(1 + \vartheta_n^\#) - \frac{\vartheta_n^\#}{(1 + \vartheta_n^\#) \ln 2} > 0$.

From (A.29), we know $r_n(p_n, B_n) \geq r_{n,e}$ ensuring (A.27) may not exist for all λ , since we do not know the range of f'_n . Whenever such $r_n(p_n, B_n) \geq r_{n,e}$ does not exist, we just define $\gamma_n(\lambda)$ as $r_{n,e}$. The above leads to the desired expression of $\gamma_n(\lambda)$ in Theorem 2 on Page 7.

We now discuss the two cases for each $n \in \mathcal{N}$:

- **Case 1:** $\tau_n^\# = 0$. In this case, (A.17) (A.19) and (A.25) mean that setting p_n , B_n , and λ as $p_n^\#$, $B_n^\#$, and $\lambda^\#$ respectively ensures (A.26) and (A.27), where we note the primal feasibility condition (4b) along with Condition 1 on Page 3 means $r_n(p_n^\#, B_n^\#) \geq r_{n,e}^{\min}$. Noting the above and (A.28), we obtain $B_n^\# = \frac{\gamma_n(\lambda^\#)}{\log_2(1+\psi_n(\lambda^\#))} \geq \frac{r_{n,e}^{\min}}{\log_2(1+\psi_n(\lambda^\#))}$.
- **Case 2:** $\tau_n^\# > 0$. In this case, (A.22) means $r_n(p_n^\#, B_n^\#) = r_{n,e}^{\min}$, which along with (A.17) and (A.25) induces $B_n^\# = \frac{r_{n,e}^{\min}}{\log_2(1+\psi_n(\lambda^\#))}$. Also, (A.19) means

$$\begin{aligned} & \nabla_{B_n} \mathcal{F}_n(p_n, B_n | \beta_n, \nu_n) |_{B_n=B_n^\#, p_n=p_n^\#} \\ &= \lambda^\# - \tau_n^\# \nabla_{B_n} r_n(p_n, B_n) |_{B_n=B_n^\#} < \lambda^\#, \end{aligned} \quad (\text{A.30})$$

where the last step uses $\tau_n^\# > 0$ and $\nabla_{B_n} r_n(p_n, B_n) |_{B_n=B_n^\#} > 0$ (note $B_n^\# > 0$ as explained in Footnote 5). The above means setting p_n , B_n , and λ as $p_n^\#$, $\frac{r_{n,e}^{\min}}{\log_2(1+\psi_n(\lambda^\#))}$, and $\lambda^\#$ respectively ensures (A.26) and (A.30). Moreover, when $\gamma_n(\lambda^\#) > 0$ exists, (A.17) (A.25) and (A.28) means setting p_n , B_n , and λ as $p_n^\#$, $\frac{\gamma_n(\lambda^\#)}{\log_2(1+\psi_n(\lambda^\#))}$, and $\lambda^\#$ respectively ensures (A.26) and (A.27). Comparing (A.27) and (A.30), and noting that

$\nabla_{B_n} \mathcal{F}_n(p_n, B_n | \beta_n, \nu_n) = \nu_n c_n f'_n(r_{n,s}(p_n, B_n)) \nabla_{B_n} r_{n,s}(p_n, B_n)$ is strictly decreasing function with respect to⁶ B_n , we obtain $B_n^\# = \frac{r_{n,e}^{\min}}{\log_2(1+\psi_n(\lambda^\#))} > \frac{\gamma_n(\lambda^\#)}{\log_2(1+\psi_n(\lambda^\#))}$. When we cannot find $\gamma_n(\lambda^\#) \geq r_{n,e}$ for (A.27), as already explained, we just set $\gamma_n(\lambda^\#)$ as $r_{n,e}$ and still have $B_n^\# = \frac{r_{n,e}^{\min}}{\log_2(1+\psi_n(\lambda^\#))} \geq \frac{\gamma_n(\lambda^\#)}{\log_2(1+\psi_n(\lambda^\#))}$ due to $r_{n,e}^{\min} \geq r_{n,e}$.

Summarizing the two cases, we conclude for any $n \in \mathcal{N}$ that

$$\begin{aligned} B_n^\# &= \max \left\{ \frac{\gamma_n(\lambda^\#)}{\log_2(1+\psi_n(\lambda^\#))}, \frac{r_{n,e}^{\min}}{\log_2(1+\psi_n(\lambda^\#))} \right\} \\ &= \frac{\max \{ \gamma_n(\lambda^\#), r_{n,e}^{\min} \}}{\log_2(1+\psi_n(\lambda^\#))}. \end{aligned} \quad (\text{A.31})$$

Then (A.29) and $r_{n,s}(p_n, B_n) = r_n(p_n, B_n) - r_{n,e}$ Now we know how to compute $B_n^\#$ in (A.31) given $\lambda^\#$. Then $\lambda^\#$ is decided such that $B_n^\# |_{n \in \mathcal{N}}$ from (A.31) together satisfy (A.23). Finally, after $\lambda^\#$ and $B_n^\#$ are obtained, $p_n^\#$ is computed as $\frac{\sigma_n^2 B_n^\# \psi_n(\lambda^\#)}{g_n}$ based on (A.17) and (A.25). To summarize, we have proved Eq. (30) of Theorem 2 on Page 7; i.e., Theorem 2 is proved. \square

For strictly concave utility, Lemma B.1 below shows that $\mathbb{P}_3(\beta, \nu)$ has a unique globally optimal solution given by Theorem 2.

LEMMA B.1. *In Theorem 2, with an additional condition that the function $f_n(x)$ for any $n \in \mathcal{N}$ is strictly concave, then Theorem 2 gives the unique globally optimal solution of $\mathbb{P}_3(\beta, \nu)$.*

PROOF. We will show the following three results, where $\Psi(\lambda)$ denotes $\sum_{n \in \mathcal{N}} \mathcal{B}_n(\lambda)$.

⁶This holds since $\nabla_{B_n} r_{n,s}(p_n, B_n)$ is strictly decreasing with respect to B_n and positive, and $f'_n(r_{n,s}(p_n, B_n))$ is non-increasing with respect to B_n and positive given Condition 2 on Page 4.

- ❶ $\Psi(\lambda)$ is strictly decreasing in $\lambda \geq 0$,
- ❷ $\lim_{\lambda \rightarrow 0^+} \Psi(\lambda) = \infty$, and
- ❸ $\lim_{\lambda \rightarrow \infty} \Psi(\lambda) = 0$.

Proving Result ❶: In Eq. (30), we also define function $\mathcal{B}_n(\lambda)$. It is used to better explain the proof here for Result (ii). Note we always enforce $\lambda \geq 0$ below. Here we consider the function $f_n(\cdot)$ for any $n \in \mathcal{N}$ is strictly concave (i.e., $f'_n(\cdot)$ is strictly decreasing) for $x \geq 0$. Combining this with the fact that $\psi_n(\lambda)$ in (A.25) is increasing in λ , we know that $\gamma_n(\lambda)$ in (30) is non-increasing in λ . Since $\psi_n(\lambda)$ is increasing and $\gamma_n(\lambda)$ is decreasing, $\mathcal{B}_n(\lambda)$ is strictly decreasing in λ , so that Result ❶ is proved.

Proving Results ❷ and ❸: Since $f'_n(x)$ here is strictly decreasing, $\gamma_n(\lambda)$ defined in (30) is at most $r_{n,e} + \zeta$ for $\zeta := (f'_n)^{-1}(\frac{\beta_n \sigma_n^2 \ln 2}{c_n g_n})$ when $\zeta \geq 0$ exists, and equals $r_{n,e}$ otherwise. Anyways, $\gamma_n(\lambda)$ is upper bounded by a constant. From (A.25), we know $\lim_{\lambda \rightarrow 0^+} \psi_n(\lambda) = 0$ and $\lim_{\lambda \rightarrow \infty} \psi_n(\lambda) = \infty$. Then from (30), we have $\lim_{\lambda \rightarrow 0^+} \mathcal{B}_n(\lambda) = 0$ and $\lim_{\lambda \rightarrow \infty} \mathcal{B}_n(\lambda) = \infty$, so that Results ❷ and ❸ are proved.

As noted in (A.25), $\lambda^\#$ is the solution of λ to $\sum_{n \in \mathcal{N}} \mathcal{B}_n(\lambda) = B_{\text{total}}$. Clearly, $\lambda^\#$ is unique given Results ❶ ❷ and ❸ above. Thus, the desired result is proved. \square

B.2 Algorithm to solve Problem $\mathbb{P}_3(\beta, \nu)$ based on Theorem 2

We still let $\Psi(\lambda)$ denote $\sum_{n \in \mathcal{N}} \mathcal{B}_n(\lambda)$. Similar to Lemma B.1 for strictly concave utility, we can prove for concave utility, $\Psi(\lambda)$ is non-increasing as λ increases. This motivates us to use the bisection method to find $\lambda^\#$ from (32).

For the bisection method, we use 0 as the initial lower bound. We can find the initial upper bound as follows. Starting with a random positive number Λ . If $\Psi(\Lambda)$ denoting $\sum_{n \in \mathcal{N}} \mathcal{B}_n(\Lambda)$ is less than B_{total} , we use Λ as the initial upper bound. If $\Psi(\Lambda)$ equals B_{total} , then Λ is just our desired $\lambda^\#$. If $\Psi(\Lambda)$ is greater than B_{total} , we check $\Psi(2\Lambda)$ denoting $\sum_{n \in \mathcal{N}} \mathcal{B}_n(2\Lambda)$. Similarly, if $\Psi(2\Lambda)$ is less than B_{total} , we use 2Λ as the initial upper bound. If $\Psi(2\Lambda)$ equals B_{total} , then 2Λ is just our desired $\lambda^\#$. If $\Psi(2\Lambda)$ is greater than B_{total} , we check $\Psi(2^2\Lambda)$ denoting $\sum_{n \in \mathcal{N}} \mathcal{B}_n(2^2\Lambda)$. The process continues. Basically, we find i such that $\Psi(2^{i-1}\Lambda)$ is greater than B_{total} , and $\Psi(2^i\Lambda)$ is less than B_{total} , then we use $2^i\Lambda$ as the initial upper bound. If there exists i which makes $\Psi(2^i\Lambda)$ equal B_{total} , then $2^i\Lambda$ is just our desired $\lambda^\#$.

With the initial lower bound and the initial upper bound explained above, the remaining process to find $\lambda^\#$ follows from the standard bisection method. In each iteration, the bisection method divides the interval $[a, b]$ in two parts by computing the midpoint $c = (a + b)/2$ of the interval and the value of $\Psi(c)$. If $\Psi(c)$ equals B_{total} , then the process has succeeded and c is just our desired $\lambda^\#$. Otherwise, if $\Psi(c)$ is greater than B_{total} , we update a to c so that the next iteration starts with the interval $[c, b]$; if $\Psi(c)$ is less than B_{total} , we update b to c so that the next iteration starts with the interval $[a, c]$. The bisection method converges when $\Psi(c)$ is close to (but should be no greater than) B_{total} .

Note that for each λ , computing $\Psi(\lambda)$ denoting $\sum_{n \in \mathcal{N}} \mathcal{B}_n(\lambda)$ costs $\mathcal{O}(N)$ time. The number of iterations to find the initial upper bound depends on the initialization, while the number of iterations for the bisection method depends on the error tolerance. With the

initial lower bound 0, the initial upper bound H , and the error tolerance ϵ , the number of iterations for the bisection method is $O(\log_2 \frac{H}{\epsilon})$.

C BASELINE ALGORITHMS FOR COMPARISON

As shown in Section 7.4, we compare our Algorithm 1 with the following baselines: ‘‘Optimizing B only’’, ‘‘Optimizing p only’’, and ‘‘Alternating optimization’’. We detail them below.

C.1 Optimizing p only

Given B_n , we define p_n^{\min} as the value of p_n which causes $r_n(p_n, B_n)$ to be r_n^{\min} . Formally,

$$p_n^{\min} := \frac{r_n^{\min}}{g_n} \text{ so that } B_n \log_2 \left(1 + \frac{g_n p_n^{\min}}{\sigma_n^2 B_n} \right) = r_n^{\min}. \quad (\text{A.32})$$

Then $r_n \geq r_n^{\min}$ in (4b) of Problem \mathbb{P}_1 means $p_n \geq p_n^{\min}$. Then ‘‘Optimizing p only’’ just means for each $n \in \mathcal{N}$, maximizing $\varphi_n(p_n, B_n)$ subject to $p_n \geq p_n^{\min}$.

LEMMA C.1. *For each $n \in \mathcal{N}$, the following results hold.*

- (i) $\varphi_n(p_n, B_n)$ is pseudoconvex and semistrictly quasiconvex for $p_n \in [p_n^{\min}, \infty)$ and $B_n \in (0, \infty)$.
- (ii) To optimize the weighted sum-UEE (which means maximizing $\varphi_n(p_n, B_n)$ given B_n for $p_n \in [p_n^{\min}, \infty)$), we just need to compute a stationary point of $\varphi_n(p_n, B_n)$ with respect to p_n given B_n and have a comparison with p_n^{\min} . The maximum of them will be a point at which $\varphi_n(p_n, B_n)$ achieves the maximum.

Given Section 7.1, below we consider $b_n = 1$, $c_n = 0$, and $d_n = 0$ so that the three types of utility functions are as follows:

- Type 1 utility function: $f_n(x) = \kappa_n \ln(1 + a_n x)$ with $\kappa_n > 0$ and $0 < a_n < 1$,
- Type 2 utility function: $f_n(x) = \kappa_n \cdot (1 - e^{-a_n x})$ with $a_n, \kappa_n > 0$,
- Type 3 utility function: $f_n(x) = \kappa_n x^{a_n}$ with $\kappa_n > 0$ and $0 < a_n < 1$.

LEMMA C.2. *For Type 1 utility function: $f_n(x) = \kappa_n \ln(1 + a_n x)$ with $\kappa_n > 0$ and $0 < a_n < 1$, $\varphi_n(p_n, B_n)$ given B_n achieves its maximum at p_n given by the maximum of the following two numbers: p_n^{\min} of Eq. (A.32), and the solution p_n to*

$$\begin{aligned} & \ln(1 + a_n \cdot (B_n \log_2(1 + \frac{g_n p_n}{\sigma_n^2 B_n}) - r_n e)) \\ & = W\left(\frac{a_n g_n B_n}{(\sigma_n^2 B_n + g_n p_n) \ln 2} \cdot (p_n + p_n^{\text{cir}})\right), \end{aligned} \quad (\text{A.33})$$

where $W(\cdot)$ is the principal branch of the Lambert W function.

LEMMA C.3. *For Type 2 utility function: $f_n(x) = \kappa_n \cdot (1 - e^{-a_n x})$ with $a_n, \kappa_n > 0$, $\varphi_n(p_n, B_n)$ given B_n achieves its maximum at p_n given by*

$$\max\{p_n^{\min} \text{ of Eq. (A.32)}, (\chi_n - 1) \frac{\sigma_n^2 B_n}{g_n}\},$$

where χ_n satisfies

$$\chi_n^{a_n B_n / (\ln 2)} e^{-a_n r_n e} + \frac{\sigma_n^2 B_n - g_n p_n^{\text{cir}}}{\chi_n \sigma_n^2 \ln 2} = \frac{a_n B_n}{\ln 2} + 1. \quad (\text{A.34})$$

LEMMA C.4. *For Type 3 utility function: $f_n(x) = \kappa_n x^{a_n}$ with $\kappa_n > 0$ and $0 < a_n < 1$, $\varphi_n(p_n, B_n)$ given B_n achieves its maximum at p_n*

being

$$\max\left\{p_n^{\min} \text{ of Eq. (A.32)}, \left[\frac{\exp\left(a_n + \frac{r_n e \ln 2}{B_n} + W\left(\left(\frac{a_n g_n p_n^{\text{cir}}}{\sigma_n^2 B_n} - a_n\right) e^{-a_n - \frac{r_n e \ln 2}{B_n}}\right) - 1\right) \frac{\sigma_n^2 B_n}{g_n}} \right]. \right. \quad (\text{A.35})$$

The proofs of Lemmas C.1, C.2, C.3, C.4 are provided in Section D below.

C.2 Optimizing B only

Given p_n , we define B_n^{\min} as the value of B_n which causes $r_n(p_n, B_n)$ to be r_n^{\min} ; i.e., $B_n^{\min} \log_2(1 + \frac{g_n p_n}{\sigma_n^2 B_n^{\min}}) = r_n^{\min}$.

Then we have the following optimization.

$$\max_{B_n} \sum_{n \in \mathcal{N}} c_n \varphi_n(p_n, B_n) \quad (\text{A.36a})$$

$$\text{subject to: } \sum_{n \in \mathcal{N}} B_n \leq B_{\text{total}}, \quad (\text{A.36b})$$

$$B_n \geq B_n^{\min}, \text{ for any } n \in \mathcal{N}. \quad (\text{A.36c})$$

From the first result of Lemma 4.6, $f_n(r_n, s(p_n, B_n))$ is concave with respect to B_n given p_n . Hence, $\varphi_n(p_n, B_n)$ is concave with respect to B_n given p_n . Then the above problem belongs to convex optimization. The Lagrange function of the problem is as follows:

$$\begin{aligned} & L(p_n, B_n, \alpha_n, \zeta) \\ & = - \sum_{n \in \mathcal{N}} c_n \varphi_n(p_n, B_n) + \sum_{n \in \mathcal{N}} \alpha_n \cdot (B_n^{\min} - B_n) \\ & \quad + \zeta \cdot (\sum_{n \in \mathcal{N}} B_n - B_{\text{total}}) \end{aligned} \quad (\text{A.37})$$

After applying KKT conditions to (A.37), we get:

$$\frac{\partial L}{\partial p_n} = -c_n \nabla_{p_n} \varphi_n(p_n, B_n) = 0 \quad (\text{A.38})$$

$$\frac{\partial L}{\partial B_n} = -c_n \nabla_{B_n} \varphi_n(p_n, B_n) - \alpha_n + \zeta = 0 \quad (\text{A.39})$$

$$\alpha_n \cdot (B_n^{\min} - B_n) = 0 \quad (\text{A.40})$$

$$\zeta \cdot (\sum_{n \in \mathcal{N}} B_n - B_{\text{total}}) = 0 \quad (\text{A.41})$$

Since $\nabla_{B_n} \varphi_n(p_n, B_n) > 0$ and $\alpha_n \geq 0$, only $\zeta > 0$ could make (A.39) hold. Hence from (A.41), we could tell that $\sum_{n \in \mathcal{N}} B_n = B_{\text{total}}$. Let $\widehat{B}_n(\zeta)$ be the solution of B_n to the following equation:

$$c_n \nabla_{B_n} \varphi_n(p_n, B_n) = \zeta. \quad (\text{A.42})$$

It is straightforward to derive the expression of $\widehat{B}_n(\zeta)$ based on (A.42). For any $x > 0$, we can prove $\log_2(1+x) - \frac{x}{(1+x) \ln 2} > 0$. Then we can prove that $\nabla_{B_n} \varphi_n(p_n, B_n)$ is decreasing as B_n increases. For each $n \in \mathcal{N}$, there are two possible cases:

- If $\alpha_n = 0$, then $B_n \geq B_n^{\min}$, $c_n \nabla_{B_n} \varphi_n(p_n, B_n) = \zeta$ so that $B_n = \widehat{B}_n(\zeta) \geq B_n^{\min}$.
- If $\alpha_n > 0$, then $B_n = B_n^{\min}$, $c_n \nabla_{B_n} \varphi_n(p_n, B_n) = \zeta - \alpha_n < \zeta$. Thus $B_n = B_n^{\min} > \widehat{B}_n(\zeta)$.

Summarizing both cases and we can derive B_n as follows:

$$B_n = \max\{\widehat{B}_n(\zeta), B_n^{\min}\} \quad (\text{A.43})$$

and ζ could be derived from:

$$\sum_{n \in \mathcal{N}} \max\{\widehat{B}_n(\zeta), B_n^{\min}\} = B_{\text{total}}. \quad (\text{A.44})$$

As $\nabla_{B_n} \varphi_n(p_n, B_n)$ is decreasing as B_n increases. Then $\widehat{B}_n(\zeta)$ decreases as ζ increases. Let $\zeta^\#$ be the solution of ζ to (A.44). We use the bisection search to find $\zeta^\#$. The following discussion is similar to that of Appendix B.2. We let $F(\zeta)$ denote $\sum_{n \in \mathcal{N}} \max\{\widehat{B}_n(\zeta), B_n^{\min}\}$. Then $F(\zeta)$ is non-increasing as ζ increases.

For the bisection method, we use 0 as the initial lower bound. We can find the initial upper bound as follows. Starting with a random positive number θ . If $F(\theta)$ is less than B_{total} , we use θ as the initial upper bound. If $F(\theta)$ equals B_{total} , then θ is just our desired $\zeta^\#$. If

$F(\theta)$ is greater than B_{total} , we check $F(2\theta)$. Similarly, if $F(2\theta)$ is less than B_{total} , we use 2θ as the initial upper bound. If $F(2\theta)$ equals B_{total} , then 2θ is just our desired $\zeta^\#$. If $F(2\theta)$ is greater than B_{total} , we check $F(2^2\theta)$. The process continues. Basically, we find i such that $F(2^{i-1}\theta)$ is greater than B_{total} , and $F(2^i\theta)$ is less than B_{total} , then we use $2^i\theta$ as the initial upper bound. If there exists i which makes $F(2^i\theta)$ equal B_{total} , then $2^i\theta$ is just our desired $\zeta^\#$.

With the initial lower bound and the initial upper bound explained above, the remaining process to find $\zeta^\#$ follows from the standard bisection method. In each iteration, the bisection method divides the interval $[a, b]$ in two parts by computing the midpoint $c = (a + b)/2$ of the interval and the value of $F(c)$. If $F(c)$ equals B_{total} , then the process has succeeded and c is just our desired $\zeta^\#$. Otherwise, if $F(c)$ is greater than B_{total} , we update a to c so that the next iteration starts with the interval $[c, b]$; if $F(c)$ is less than B_{total} , we update b to c so that the next iteration starts with the interval $[a, c]$. The bisection method converges when $F(c)$ is close to (but should be no greater than) B_{total} .

After using the bisection method to find $\zeta^\#$, we compute B_n as $\max\{\widehat{B}_n(\zeta^\#), B_n^{\min}\}$ for each $n \in \mathcal{N}$.

C.3 Alternating optimization

The algorithm for alternating optimization is to combine the algorithms of “optimizing \mathbf{p} only” in C.1 and “optimizing \mathbf{B} only” in C.2 to perform optimization in an alternating manner.

Specifically, we treat “optimizing p_n only” first and then “optimizing B_n only” as a round. After each round, we will compare the new solution with that of the last round. If the relative difference between them is less than our pre-determined threshold, we consider that alternating optimization of \mathbf{p} and \mathbf{B} has converged.

D PROOF OF LEMMAS FOR APPENDIX C

D.1 Proof of Lemma C.1

We first have the following properties of $\varphi_n(p_n, B_n)$.

- From Lemma 4.6, the numerator $f_n(r_{n,s}(p_n, B_n))$ of $\varphi_n(p_n, B_n)$ is jointly concave in p_n and B_n . Then from Result (iii) of Theorem 2.3.8 in [19], $\varphi_n(p_n, B_n)$ is semistrictly quasiconcave which means that Result (i) of Lemma C.1 is proved, where the definition of “semistrictly quasiconcave” is provided in Footnote 7.
- From Lemma 2.2 of [37], a scalar function $g(\cdot)$ over a convex set \mathcal{X} is semistrictly quasiconcave if and only if any closed segment $\mathcal{S} \subset \mathcal{X}$ can be split into three segments $\mathcal{S}_1, \mathcal{S}_2, \mathcal{S}_3$ such that $g(\cdot)$ is increasing in \mathcal{S}_1 , constant in \mathcal{S}_2 , and decreasing in \mathcal{S}_3 . Note that $\mathcal{S}_1, \mathcal{S}_2, \mathcal{S}_3$ can be \emptyset .

Then we define p_n^{sec} as the transmission power as:

$$p_n^{\text{sec}} := \frac{r_{n,e}}{g_n} \text{ so that } B_n \log_2\left(1 + \frac{g_n p_n^{\text{sec}}}{\sigma_n^2 B_n}\right) = r_{n,e}. \quad (\text{A.45})$$

Combining the above with Eq. (3), we could derive that: $\varphi_n(p_n^{\text{sec}}, B_n) = 0$, $\lim_{p_n \rightarrow \infty} \varphi_n(p_n, B_n) = 0$, and $\varphi_n(p_n, B_n) > 0$ for $p_n \in (p_n^{\text{sec}}, \infty)$,

⁷Theorem 2.3.8 of [19] and Lemma 2.2 of [37] are about “semistrictly quasiconvex”, but can easily be extended to “semistrictly quasiconcave” since a function $g(\cdot)$ is semistrictly quasiconvex if and only if $-g(\cdot)$ is semistrictly quasiconcave. Specifically, a function $g(\cdot)$ is semistrictly quasiconvex (resp., semistrictly quasiconcave) if and only if for any x, y , the result $g(y) < g(x)$ (resp., $g(y) > g(x)$) implies that $g(x+t(y-x))$ is smaller (resp., greater) than $g(x)$ for any $t \in (0, 1)$.

we know that⁸ there exists \widehat{p}_n and \widetilde{p}_n (possibly the same) such that $\varphi_n(p_n, B_n)$ is increasing in $[p_n^{\text{sec}}, \widehat{p}_n]$, constant in $[\widehat{p}_n, \widetilde{p}_n]$, and decreasing in $[\widetilde{p}_n, \infty)$.

The condition $r_n^{\min} \geq r_{n,e}$ means $p_n^{\min} \geq p_n^{\text{sec}}$. Hence, the above analysis induces the following cases.

- If $p_n^{\min} < \widehat{p}_n$, then $\varphi_n(p_n, B_n)$ is increasing in $[p_n^{\min}, \widehat{p}_n]$, constant in $[\widehat{p}_n, \widetilde{p}_n]$, and decreasing in $[\widetilde{p}_n, \infty)$.
- If $\widehat{p}_n \leq p_n^{\min} \leq \widetilde{p}_n$, then $\varphi_n(p_n, B_n)$ is constant in $[\widehat{p}_n, \widetilde{p}_n]$, and decreasing in $[\widetilde{p}_n, \infty)$.
- If $\widetilde{p}_n < p_n^{\min}$, then $\varphi_n(p_n, B_n)$ is decreasing in $[p_n^{\min}, \infty)$.

Based on the above, Result (ii) of Lemma C.1 is also proved. \square

D.2 Proof of Lemma C.2

Given Section 7.1, we consider $b_n = 1$ so that Type 1 utility function is $f_n(x) = \kappa_n \ln(1 + a_n x)$ with $\kappa_n > 0$ and $0 < a_n < 1$.

We write $r_{n,s}(p_n, B_n)$ as $r_{n,s}$ for simplicity below. Given B_n , by letting the derivative of $\varphi_n(p_n, B_n)$ with respect to p_n be zero, we obtain

$$\frac{\kappa_n a_n}{1 + a_n r_{n,s}} \cdot (\nabla_{p_n} r_{n,s}) \cdot (p_n + p_n^{\text{cir}}) = \kappa_n \ln(1 + a_n r_{n,s}), \quad (\text{A.46})$$

which induces

$$a_n \cdot (\nabla_{p_n} r_{n,s}) \cdot (p_n + p_n^{\text{cir}}) = (1 + a_n r_{n,s}) \ln(1 + a_n r_{n,s}). \quad (\text{A.47})$$

This means

$$\ln(1 + a_n r_{n,s}) = W(a_n \cdot (\nabla_{p_n} r_{n,s}) \cdot (p_n + p_n^{\text{cir}})), \quad (\text{A.48})$$

for $W(\cdot)$ being the principal branch of the Lambert W function; i.e., $W(z)$ for $z \geq -e^{-1}$ is the solution of $x \geq -1$ to the equation $x e^x = z$.

From $r_{n,s}(p_n, B_n) := B_n \log_2(1 + \frac{g_n p_n}{\sigma_n^2 B_n}) - r_{n,e}$, we have

$$\begin{aligned} & (\nabla_{p_n} r_{n,s}) \cdot (p_n + p_n^{\text{cir}}) \\ &= \frac{\frac{g_n}{\sigma_n^2}}{(1 + \frac{g_n p_n}{\sigma_n^2 B_n}) \ln 2} \cdot (p_n + p_n^{\text{cir}}) \\ &= \frac{g_n B_n}{(\sigma_n^2 B_n + g_n p_n) \ln 2} \cdot (p_n + p_n^{\text{cir}}). \end{aligned} \quad (\text{A.49})$$

Then we can solve

$$\begin{aligned} & \ln(1 + a_n \cdot (B_n \log_2(1 + \frac{g_n p_n}{\sigma_n^2 B_n}) - r_{n,e})) \\ &= W\left(\frac{a_n g_n B_n}{(\sigma_n^2 B_n + g_n p_n) \ln 2} \cdot (p_n + p_n^{\text{cir}})\right). \end{aligned} \quad (\text{A.50})$$

Using Result (ii) of Lemma C.1, the optimal p_n given B_n for the weighted sum-UEE optimization is given by the maximum of the following two numbers: p_n^{\min} of Eq. (A.32), and the solution p_n to the above Eq. (A.50). \square

D.3 Proof of Lemma C.3

Given Section 7.1, we consider $c_n = 0$ so that Type 2 utility function is $f_n(x) = \kappa_n \cdot (1 - e^{-a_n x})$ with $a_n, \kappa_n > 0$.

We write $r_{n,s}(p_n, B_n)$ as $r_{n,s}$ for simplicity below. Given B_n , by letting the derivative of $\varphi_n(p_n, B_n)$ with respect to p_n be zero, we obtain

$$\kappa_n a_n e^{-a_n r_{n,s}} (\nabla_{p_n} r_{n,s}) \cdot (p_n + p_n^{\text{cir}}) = \kappa_n \cdot (1 - e^{-a_n r_{n,s}}), \quad (\text{A.51})$$

which induces

$$a_n \cdot (\nabla_{p_n} r_{n,s}) \cdot (p_n + p_n^{\text{cir}}) = e^{a_n r_{n,s}} - 1. \quad (\text{A.52})$$

⁸For the specific types of utility functions $f_n(\cdot)$ used in Section 7.1 of this paper, we can show $\widehat{p}_n = \widetilde{p}_n$ in principle, but it is not the focus of our paper and does not impact the validity of our results.

With $\chi_n := 1 + \frac{g_n p_n}{\sigma_n^2 B_n}$, we further obtain

$$\begin{aligned} & (\nabla_{p_n} r_{n,s}) \cdot (p_n + p_n^{\text{cir}}) \\ &= \frac{\frac{g_n}{\sigma_n^2}}{(1 + \frac{g_n p_n}{\sigma_n^2 B_n}) \ln 2} \cdot (p_n + p_n^{\text{cir}}) \\ &= \frac{(\chi_n - 1) \sigma_n^2 B_n + g_n p_n^{\text{cir}}}{\chi_n \sigma_n^2 \ln 2} \\ &= \frac{B_n}{\ln 2} + \frac{g_n p_n^{\text{cir}} - \sigma_n^2 B_n}{\chi_n \sigma_n^2 \ln 2}. \end{aligned} \quad (\text{A.53})$$

Then

$$\begin{aligned} & a_n \cdot \left(\frac{B_n}{\ln 2} + \frac{g_n p_n^{\text{cir}} - \sigma_n^2 B_n}{\chi_n \sigma_n^2 \ln 2} \right) \\ &= e^{a_n B_n \log_2 \chi_n} e^{-a_n r_{n,e}} - 1 \\ &= \chi_n^{a_n B_n / (\ln 2)} e^{-a_n r_{n,e}} - 1. \end{aligned} \quad (\text{A.54})$$

We further get

$$\chi_n^{a_n B_n / (\ln 2)} e^{-a_n r_{n,e}} + \frac{\sigma_n^2 B_n - g_n p_n^{\text{cir}}}{\chi_n \sigma_n^2 \ln 2} = a_n \frac{B_n}{\ln 2} + 1. \quad (\text{A.55})$$

Using Result (ii) of Lemma C.1, the optimal p_n given B_n for the weighted sum-UEE optimization is given by the maximum of the following two numbers: p_n^{\min} of Eq. (A.32), and $(\chi_n - 1) \frac{\sigma_n^2 B_n}{g_n}$, where χ_n is the solution to the above Eq. (A.55). \square

D.4 Proof of Lemma C.4

Given Section 7.1, we consider $d_n = 0$ so that Type 3 utility function is $f_n(x) = \kappa_n x^{a_n}$ with $\kappa_n > 0$ and $0 < a_n < 1$.

We write $r_{n,s}(p_n, B_n)$ as $r_{n,s}$ for simplicity below. Given B_n , by letting the derivative of $\varphi_n(p_n, B_n)$ with respect to p_n be zero, we obtain

$$\kappa_n a_n r_{n,s}^{a_n - 1} \cdot (\nabla_{p_n} r_{n,s}) \cdot (p_n + p_n^{\text{cir}}) = \kappa_n r_{n,s}^{a_n}. \quad (\text{A.56})$$

Then we have

$$a_n \cdot (\nabla_{p_n} r_{n,s}) \cdot (p_n + p_n^{\text{cir}}) = r_{n,s}. \quad (\text{A.57})$$

From $r_{n,s}(p_n, B_n) := B_n \log_2(1 + \frac{g_n p_n}{\sigma_n^2 B_n}) - r_{n,e}$, we have

$$\nabla_{p_n} r_{n,s} = \frac{\frac{g_n}{\sigma_n^2}}{(1 + \frac{g_n p_n}{\sigma_n^2 B_n}) \ln 2}, \quad (\text{A.58})$$

which is used in (A.57) so that

$$a_n \cdot \frac{\frac{g_n}{\sigma_n^2}}{(1 + \frac{g_n p_n}{\sigma_n^2 B_n}) \ln 2} \cdot (p_n + p_n^{\text{cir}}) = B_n \log_2(1 + \frac{g_n p_n}{\sigma_n^2 B_n}) - r_{n,e}. \quad (\text{A.59})$$

With $\chi_n := 1 + \frac{g_n p_n}{\sigma_n^2 B_n}$, we further obtain

$$a_n \cdot \frac{\frac{g_n}{\sigma_n^2}}{\chi_n} \left((\chi_n - 1) \frac{\sigma_n^2 B_n}{g_n} + p_n^{\text{cir}} \right) + r_{n,e} \ln 2 = B_n \ln \chi_n, \quad (\text{A.60})$$

which is simplified as

$$a_n + \frac{r_{n,e} \ln 2}{B_n} + \left(\frac{a_n g_n p_n^{\text{cir}}}{\sigma_n^2 B_n} - a_n \right) \frac{1}{\chi_n} = \ln \chi_n. \quad (\text{A.61})$$

Then it follows that

$$\chi_n = \exp \left(a_n + \frac{r_{n,e} \ln 2}{B_n} + \left(\frac{a_n g_n p_n^{\text{cir}}}{\sigma_n^2 B_n} - a_n \right) \exp \left(-a_n - \frac{r_{n,e} \ln 2}{B_n} \right) \right). \quad (\text{A.62})$$

Using Result (ii) of Lemma C.1, the optimal p_n given B_n for the weighted sum-UEE optimization is given by the maximum of the following two numbers: p_n^{\min} of Eq. (A.32), and $(\chi_n - 1) \frac{\sigma_n^2 B_n}{g_n}$, where χ_n is given by the above Eq. (A.62). \square

E ADDITIONAL SIMULATION RESULTS

We provide more simulation results here. Note that our theoretical analysis and simulation results apply to uplink communications as well as downlink communications. For downlink communications, the circuit power p_n^{cir} in the denominator $p_n + p_n^{\text{cir}}$ of (3) is the additional power that the server consumes to transmit signals with power p_n to user U_n , and it is possible that p_n^{cir} can be the same for different n for such downlink communications. As noted in Section 7.3, the simulations set the circuit power p_n^{cir} as 2 dBm (i.e., 1.6 milliwatts) for each n .

E.1 Impact by the number of users

We compare the UEE under different numbers of users N : 10, 20, 30, 40, and 50 under three different user scenarios (i.e., three utility functions in Fig. 2(a)). Fig. 6(a) shows how the sum-UEE changes with the increase of the number of users N . It could be seen that as N becomes larger, the sum-UEE also increases. They are positively correlated. In contrast, the average UEE tends to decrease as the number of users N increases, which could be seen in Fig. 6(b). That is due to a reduction in the bandwidth allocated to each user.

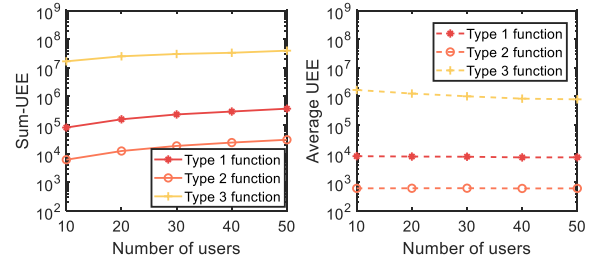


Figure 6: (a). Sum-UEE under different N . (b). Average UEE under different N .

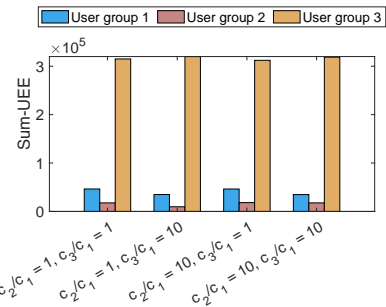


Figure 7: Sum-UEE of each user group with different priorities and utility functions. The utility functions are obtained from the table results in Section 7.2 with the SSV360 dataset [33]. User group 1 uses $f_n(r_{n,s}) = 0.5424 \ln(1 + 37.2965 r_{n,s})$. User group 2 uses $f_n(r_{n,s}) = 2.9351(1 - e^{-2.1224 r_{n,s}})$. User group 3 uses $f_n(r_{n,s}) = 3.2956(r_{n,s}/15.94)^{0.2733}$.

E.2 Heterogeneous types of utility functions among the users

We use Figure 7 to show that our studied system and proposed algorithm allow heterogeneous types of utility functions among the users. We consider that 30 users are evenly classified into three priority levels, corresponding to different weights c_n . Larger c_n means more weight in our studied optimization. For example, the legend “ $c_2/c_1 = a, c_3/c_1 = b$ ” in Fig. 7 means 10 users in Group 1 with weight c_1 , 10 users in Group 2 with weight ac_1 , and 10 users in Group 3 with weight bc_1 . In Figure 7, we can see that with a fixed c_2/c_1 , increasing c_3/c_1 will improve Group 3’s sum-UEE, and reduce Group 1’s and 2’s sum-UEE; with a fixed c_3/c_1 , enlarging c_2/c_1 will enhance Group 2’s sum-UEE, and shrink Group 1’s and 3’s sum-UEE. The above simulation results are consistent with the intuition.

F USING OUR TECHNIQUE FOR GLOBAL OPTIMIZATION OF FRACTIONAL PROGRAMMING

Two recent papers [26, 27] by Shen and Yu are well-cited and have been considered breakthroughs in fractional programming. However, their proposed technique finds neither locally nor globally optimal solution. In contrast, with our technique of Section 6, a globally optimal solution can be found. The following problem is considered by Shen and Yu [26, 27].

The following problem \mathbb{P}_4 is considered by Shen and Yu [26, 27], where $A_n(\cdot), B_n(\cdot), C(\cdot), g_m(\cdot)$, and $h_\ell(\cdot)$ are functions, with $A_n(\mathbf{x}) > 0$ and $B_n(\mathbf{x}) > 0$ for all $n = 1, 2, \dots, N$.

$$\text{Problem } \mathbb{P}_4: \min_{\mathbf{x} \in \mathbb{R}^J} C(\mathbf{x}) + \sum_{n=1}^N \frac{A_n(\mathbf{x})}{B_n(\mathbf{x})} \quad (\text{A.63})$$

$$\text{subject to: } g_m(\mathbf{x}) \leq 0, \text{ for } m = 1, 2, \dots, M, \quad (\text{A.63a})$$

$$h_\ell(\mathbf{x}) = 0, \text{ for } \ell = 1, 2, \dots, L. \quad (\text{A.63b})$$

We introduce an auxiliary variable α_n to transform Problem \mathbb{P}_4 into the epigraph form. Let $\alpha_n \geq \frac{A_n(\mathbf{x})}{B_n(\mathbf{x})}$ and \mathbb{P}_4 can be transformed to the following equivalent form as \mathbb{P}_5 :

$$\text{Problem } \mathbb{P}_5: \min_{\mathbf{x} \in \mathbb{R}^J, \alpha \in \mathbb{R}^N} C(\mathbf{x}) + \sum_{n=1}^N \alpha_n \quad (\text{A.64})$$

$$\text{subject to: } A_n(\mathbf{x}) - \alpha_n B_n(\mathbf{x}) \leq 0, \text{ for } n = 1, 2, \dots, N, \quad (\text{A.64a})$$

$$g_m(\mathbf{x}) \leq 0, \text{ for } m = 1, 2, \dots, M, \quad (\text{A.64b})$$

$$h_\ell(\mathbf{x}) = 0, \text{ for } \ell = 1, 2, \dots, L, \quad (\text{A.64c})$$

Similar to how we connect \mathbb{P}_2 and $\mathbb{P}_3(\boldsymbol{\beta}, \boldsymbol{\nu})$ in Section 5.1, we can connect \mathbb{P}_5 and $\mathbb{P}_6(\boldsymbol{\alpha}, \boldsymbol{\beta})$ defined as follows:

Problem $\mathbb{P}_6(\boldsymbol{\alpha}, \boldsymbol{\beta})$:

$$\min_{\mathbf{x} \in \mathbb{R}^J} C(\mathbf{x}) + \sum_{n=1}^N \alpha_n + \sum_{n=1}^N \beta_n \cdot (A_n(\mathbf{x}) - \alpha_n B_n(\mathbf{x})) \quad (\text{A.65})$$

$$\text{subject to: } g_m(\mathbf{x}) \leq 0, \text{ for } m = 1, 2, \dots, M, \quad (\text{A.65a})$$

$$h_\ell(\mathbf{x}) = 0, \text{ for } \ell = 1, 2, \dots, L, \quad (\text{A.65b})$$

If $A_n(\cdot), C(\cdot), g_m(\cdot)$ are convex, $B_n(\cdot)$ is concave, and h_ℓ is affine, then $\mathbb{P}_6(\boldsymbol{\alpha}, \boldsymbol{\beta})$ belongs to convex optimization.

The solving process of \mathbb{P}_5 (i.e., \mathbb{P}_4) is transformed into solving a series of parametric convex optimization $\mathbb{P}_6(\boldsymbol{\alpha}, \boldsymbol{\beta})$ where $[\boldsymbol{\alpha}, \boldsymbol{\beta}]$ is

given so that there is no non-convex product term $\alpha_n B_n(\mathbf{x})$. The solving of each \mathbb{P}_6 is used to update $[\boldsymbol{\alpha}, \boldsymbol{\beta}]$ under which \mathbb{P}_6 is solved again with the new $[\boldsymbol{\alpha}, \boldsymbol{\beta}]$, where the update of $[\boldsymbol{\alpha}, \boldsymbol{\beta}]$ is based on the KKT conditions of \mathbb{P}_5 . The process is similar to what we have presented in Section 5.1 for \mathbb{P}_2 and $\mathbb{P}_3(\boldsymbol{\beta}, \boldsymbol{\nu})$.